2016

Evaluating Steel Byproducts and Natural Minerals for Phosphate Adsorption from Agricultural Subsurface Drainage

Bjorn Sellner
South Dakota State University, bjornsellner@hotmail.com

EVALUATING STEEL BYPRODUCTS AND NATURAL MINERALS FOR PHOSPHATE ADSORPTION FROM AGRICULTURAL SUBSURFACE DRAINAGE

BY

BJORN SELLNER

A thesis submitted in partial fulfillment of the requirements for the

Master of Science

Major in Civil Engineering

South Dakota State University

2016

EVALUATING STEEL BYPRODUCTS AND NATURAL MINERALS FOR PHOSPHATE ADSORPTION FROM AGRICULTURAL SUBSURFACE DRAINAGE

This thesis is approved as a creditable and independent investigation by a candidate for the Master of Science in Civil Engineering degree and is acceptable for meeting the thesis requirements for this degree. Acceptance of this does not imply that the conclusions reached by the candidate are necessarily the conclusions of the major department.

Guanghui Hua, Ph.D.
Thesis Advisor Date

Nadim Wehbe, Ph.D.
Head, Department of Civil and Environmental Engineering Date

Dean, Graduate School Date

ACKNOWLEDGEMENTS

Thank you to my research advisor Dr. Guanghui Hua for your continuous support and guidance over the past two years. You have helped develop many of my skills and prepared me for my future endeavors. I would also like to thank all of the professors in the Civil and Environmental Engineering Department and the Agricultural and Biosystems Engineering Department at South Dakota State University for their impartment of knowledge and support. I would like to thank my family and friends for their constant encouragement. Thank you to Prairie Manufacturing, LLC (Sioux Falls, SD), Nucor Corporation (Norfolk, NE), and Martin Marietta Aggregates (Fort Dodge, IA) for generously providing testing materials for this project. I would also like to thank the South Dakota Soybean Research and Promotion Council for funding this work.

CONTENTS

LIST OF ABBREVIATIONS

Al	Aluminum
C/C_0	Ratio of outlet P to inlet P
C_e	Equilibrium P concentration
C_0	Initial P concentration
Ca	Calcium
$CaCO_3$	Calcium carbonate
Cu	Copper
DOC	Dissolved organic carbon
EBCT	Empty bed contact time
Fe	Iron
ΔG°	Gibb's free energy change
ΔH°	Enthalpy change
HA	Humic acid
HCl	Hydrochloric acid
K_F	Freundlich constant
K_L	Langmuir constant
k_1	Pseudo first-order equilibrium rate constant
k_2	Pseudo second-order equilibrium rate constant
KCl	Potassium chloride
NaOH	Sodium hydroxide
NO_3^--N	Nitrate as nitrogen
OH^-	Hydroxide

P	Phosphorus
PO_4^{3-}-P	Phosphate as P
q_e	Equilibrium P adsorption capacity
q_{max}	Maximum P adsorption capacity
q_t	Time specific P adsorption capacity
q_{total}	Total mass of P adsorbed
Q	Volumetric flow rate
R	Universal gas constant
rpm	Rotations per minute
ΔS°	Entropy change
SO_4^{2-}	Sulfate
T	Temperature
WC	Woodchip
Zn	Zinc

LIST OF FIGURES

LIST OF TABLES

ABSTRACT

EVALUATING STEEL BYPRODUCTS AND NATURAL MINERALS FOR PHOSPHATE ADSORPTION FROM AGRICULTURAL SUBSURFACE DRAINAGE

BJORN SELLNER

2016

The loss of phosphorus (P) from agricultural soils to surface waters is recognized as a key contributing factor to eutrophication in surface waters. Recent studies have shown that in addition to surface runoff, subsurface drainage can contribute substantially to the loss of P from soils. The use of adsorption materials to bind P has emerged as a promising technology for P removal. The objective of this study was to perform batch and column experiments to investigate the P adsorption potential of several materials for agricultural subsurface drainage treatment.

Laboratory batch adsorption experiments were performed to determine the P adsorption capacities of natural minerals and industrial byproducts, including limestone, zeolite, calcite, steel slag, iron filings, and steel byproducts. Steel byproducts are a low-cost, readily available material that has high P adsorption potential. The steel byproducts included small chips, medium chips, and large turnings, which were collected from local machine shops. The impact of temperature, reaction time, pH, nitrate, sulfate, and dissolved organic carbon (DOC) on the adsorption of P were evaluated for this study. The results showed that iron-based industrial byproducts had adsorption capacities that are one order of magnitude higher than natural minerals. The three sizes of steel byproducts exhibited P adsorption capacities of 2.54 to 4.47 mg/g, which were comparable to the steel slag and the iron filings. The P adsorption capacity increased by factors of 1.2 to 2.8 when increasing temperatures from 5 to 30 °C for the selected materials. Steel byproducts

exhibited fast P adsorption kinetics as more than 60% of the 24 h adsorption potential occurred within 8 h. Decreasing pH resulted in an increased adsorption capacity among steel byproducts. Nitrate and sulfate had little impact on P removal for steel byproducts while DOC inhibited P adsorption by up to 24%.

Laboratory fixed-bed column adsorption experiments were performed to determine the P adsorption characteristics of steel byproducts and steel slag. The steel byproducts included small chips, medium chips, and large chips. The impact of initial P concentration, empty bed contact time (EBCT), pH, and DOC on the adsorption of P were evaluated for this study. The potential for P recovery by desorption and the ability to remove other contaminants was also investigated. The results showed that steel byproducts had cumulative P removals of 8.43 to 10.4 mg/g over 4800 empty bed volumes, while steel slag only removed 1.50 mg/g before exhaustion. Based on the results, medium steel chips were chosen for further testing. Higher initial P concentrations resulted in faster exhaustion and longer EBCTs increased P removal efficiencies and P adsorption capacities. Decreasing pH from 9.0 to 5.0 resulted in an increase in P adsorption by 56% for medium steel chips. DOC inhibited P adsorption by up to 38%. Recoveries of 59 to 83% of the attached P were measured using varying strengths of NaOH solution. Medium steel chips removed considerable amount of DOC, Cu, and Zn along with P in a mixed contaminant study. Overall, the results of this study suggest that steel byproducts are an efficient P adsorption material that can potentially be used for agricultural subsurface drainage treatment.

CHAPTER 1
INTRODUCTION

The installation of subsurface drainage in poorly drained agricultural fields is a common practice in the Midwestern United States and many other areas (Fausey et al. 1995). Subsurface drainage systems are composed of a network of perforated pipes buried underneath the soil, which remove excess water from the soil profile, increasing and providing more uniform crop production (Zucker and Brown 1998). However, the increase in water infiltration facilitates the transport of soil-applied nutrients to subsurface drains, which provide a direct pathway for nutrients to nearby water bodies (Fausey et al. 1995; King et al. 2015). Consequently, the excess nutrient loading on surface waters can lead to eutrophication, resulting in algal blooms, anoxia, and loss of aquatic life (Correll 1998).

Phosphorus (P) is typically the limiting nutrient in freshwater ecosystems, with total P concentrations $\geq$ 0.02 mg/L a concern for the development of eutrophic conditions (Correll 1998; Heathwaite and Dils 2000). Historically, surface runoff has been recognized as the primary mechanism for P transport from agricultural fields to surface water bodies (Baker et al. 1975; Sharpley et al. 1994). However, recent studies have found that P loss via subsurface drainage is substantial, especially in soils with low P sorption capacities (Sims et al. 1998). Furthermore, P losses in subsurface drainage are typically dominated by dissolved P, which is 100% biologically available for uptake (Algoazany et al. 2007; Hansen et al. 2002). P concentrations well in exceedance of the 0.02 mg P/L threshold have been reported in subsurface drains across the Midwestern United States (Gentry et al. 2007; King et al. 2015).

In order to prevent further damage to surface water ecosystems, it is crucial to develop best management practices to mitigate P losses from agricultural subsurface drainage. Adsorption onto various natural minerals, industrial byproducts, and commercial products has emerged as an effective P removal technique for the treatment of several types of polluted waters (Chardon et al. 2012; Erickson et al. 2007; Stoner et al. 2012). The goal of this study was to evaluate several natural minerals and industrial byproducts for P adsorption in batch and column settings and determine their applicability for agricultural subsurface drainage treatment. A special focus of this study was evaluating steel byproducts as a potential adsorption material. Steel byproducts are a promising new Fe-based material that is readily available in many areas, inexpensive, and has high P removal potential. Chapter 2 is titled "Evaluating Industrial Byproducts and Natural Minerals for Phosphate Adsorption from Agricultural Subsurface Drainage". Chapter 2 discusses batch P adsorption experiments investigating the effects of temperature, time, pH, coexisting substances, and real drainage matrixes on the P removal performance or several natural minerals and industrial byproducts. Chapter 3 is titled "Adsorption of Phosphate Using Steel Byproducts to Treat Agricultural Subsurface Drainage: A Fixed-Bed Column Study". Chapter 3 discusses column P adsorption experiments specifically focusing on steel byproducts as an adsorbent. Chapter 4 contains a summary of the results found in Chapters 2 and 3 and provides recommendations for future testing.

CHAPTER 2
EVALUATING INDUSTRIAL BYPRODUCTS AND NATURAL MINERALS FOR PHOSPHATE ADSORPTION FROM AGRICULTURAL SUBSURFACE DRAINAGE

2.1 Introduction

The installation of subsurface drainage in poorly drained agricultural fields is a common practice in the Midwestern United States and many other areas (Fausey et al. 1995). Subsurface drainage has made farming possible in an estimated 25% of cropland in the United States and Canada (Skaggs et al. 1994) and increased yields by 5 to 25% in certain areas (Eidman 1997) by lowering shallow water tables to remove excess soil moisture. However, subsurface drainage provides a direct pathway for nutrients to be transported to surface waters (Fausey et al. 1995). Excess nutrient loading on surface waters can accelerate the eutrophication process, leading to diminished water quality, poisonous algal blooms, anoxia, and loss of aquatic life (Sharpley and Tunney 2000).

Phosphorus (P) has been identified to generally be the limiting nutrient in surface waters and excess total P concentrations $\geq$ 0.02 mg/L are often considered problematic (Correll 1998; Schindler et al. 2008). In agricultural landscapes, the two primary pathways for P transport are surface runoff and subsurface flow. Early work identified surface runoff as the primary method of P transport and P contributions from subsurface flow were often deemed negligible due to low concentrations and the ability for subsoil to bind P (Baker et al. 1975). However, recent work has found subsurface drainage to be a significant pathway for P export to receiving water bodies (Gentry et al. 2007; King et al. 2015; Smith et al. 2015; Zhang et al. 2015). Subsurface drainage is typically dominated by dissolved P, which is 100% biologically available for aquatic life (Sonzogni et al.

1982). In an eight year study, King et al. (2015) determined that subsurface drainage accounted for 48% of dissolved P exported from a watershed in central Ohio, and greater than 90% of the measured concentrations exceeded the 0.02 mg/L threshold. In three central Illinois watersheds, Gentry et al. (2007) measured dissolved P concentrations as high as 1.25 mg/L discharged from subsurface drainage. To mitigate P loss and prevent further damage to surface water ecosystems, management practices must be developed to remove P from agricultural subsurface drainage.

Adsorption of P onto low-cost materials has emerged as a promising technology for P removal from various types of polluted waters (Chardon et al. 2012; Erickson et al. 2007; Stoner et al. 2012). Several natural minerals, industrial byproducts, and synthetic products have been evaluated to determine their potential to adsorb P including limestone, olivine, zeolite, steel slag, fly ash, iron filings, granular activated carbon, Filtralite-P®, and others (Adam et al. 2007; Erickson et al. 2007; Hussain et al. 2011; Oguz 2004; Penn et al. 2011; Reddy et al. 2014) Typically, materials rich in calcium (Ca), aluminum (Al), and iron (Fe) have been used because of their ability to provide a cation for P to react with, creating an insoluble compound (Buda et al. 2012; Lyngsie et al. 2014). A promising new iron-based adsorption media are carbon steel byproducts. Collected from machine shops, these typically recycled or landfilled byproducts are composed of various sizes of chips and turnings that have the potential to adsorb significant amounts of P. As Fe oxidizes to form rust, the Fe oxides have the ability to remove P from solution via ligand exchange, electrostatic adsorption, and the formation of Fe-P precipitates (Allred and Racharaks 2014). Because of their expected high adsorption capacities and potential for use as a low-cost new media to remove P from

subsurface drainage, steel byproducts were chosen for batch testing among other previously studied natural minerals and industrial byproducts.

The objective of this study was to investigate the P adsorption characteristics of selected natural minerals and industrial byproducts including limestone, zeolite, calcite, steel slag, iron filings, and steel byproducts and determine their potential for subsurface drainage treatment. Batch experiments were conducted to determine the P adsorption capacities of selected materials, including the effect of temperature, time, pH, coexisting substances, and real drainage matrixes. The desorbability of attached P from the materials was also investigated. A special focus of this study was to evaluate steel byproducts as potential low-cost and readily available P adsorption materials for subsurface drainage treatment.

2.2 Materials and Methods

2.2.1 Adsorbents

Three natural materials and five industrial byproducts were characterized and tested for P adsorption in batch conditions. These materials include limestone, zeolite, calcite, electric arc furnace steel slag, iron filings, and three sizes of carbon steel byproducts. Limestone is a sedimentary rock that is largely composed of calcium carbonate ($CaCO_3$) and it was obtained from Martin Marietta Aggregates (Fort Dodge, IA). Zeolite is an aluminosilicate mineral that has been used for ion-exchange water treatment and it was obtained from Bear River Zeolite Co., Inc. (Preston, ID). Calcite is a pure form of $CaCO_3$, typically used as a pH neutralizer and was obtained from Fresh Water Systems (Greenville, SC). Electric arc furnace steel slag is a byproduct of the steel

making industry produced when scrap metal and fluxes are oxidized by the use of an electric current and contains Ca, Al, and Fe. The steel slag was obtained from Nucor Corporation (Norfolk, NE). Iron filings are a product of grinding, milling, or filing of finished iron products and were obtained from Connelly-GPM, Inc. (Chicago, IL). Steel byproducts are produced from machine shops by cutting, shaping, drilling, and finishing carbon steel products. The steel byproducts tested are graded as 1018 carbon steel and were obtained from Prairie Manufacturing, LLC (Sioux Falls, SD).

All eight materials were washed with deionized water to remove dirt and fines present. To remove any oil that may have been on the surface, iron filings and the steel byproducts were also washed with phosphate-free soap. Washed materials were air dried overnight. During the drying process, the steel byproducts oxidized, forming a layer of rust on the surface. After drying, the materials were sieved to a desired size range and subjected to physical and chemical characterization tests based on American Society of Testing and Materials (ASTM) standard testing procedures. The physical and chemical properties of the materials are shown in Table 2.1. For comparison purposes, limestone, zeolite, and calcite were sieved to a size range of 0.9-2.0 mm. To identify the impact of particle size on P adsorption, the steel byproducts were sorted and sieved to three sizes including small steel chips (0.1-2.0 mm), medium steel chips (2.0-4.8 mm), and large steel turnings (10-30 mm). Iron filings and steel slag were sieved to sizes comparable to small steel chips and medium steel chips, respectively. Particle densities for the eight materials were measured as the amount of water volume displaced by a certain mass of material. Fe-based products had high particle densities between 5.20-5.91 g/cm^3, while steel slag and natural minerals had lower particle densities between 2.18-3.57 g/cm^3.

Moisture content and organic content were measured using ASTM D2974, and pH values were determined using ASTM D4972. The four Fe-based adsorbents had material pH values that were slightly acidic ($\leq$ 6.5) while steel slag and the three natural minerals were alkaline ($\geq$ 8.0). Zeolite and steel slag had moisture contents of 3.2 and 0.7% and organic contents of 2.0 and 4.7%, respectively. Moisture content and organic content were zero in all other materials, except limestone and calcite, which had organic content that ranged from 0.4 and 0.8%, respectively.

2.2.2 General Batch Adsorption

Phosphorus stock solution was prepared by dissolving monopotassium phosphate (KH_2PO_4) in deionized water. For each experiment, 0.5 g (iron filings and small steel chips), 1.0 g (steel slag, medium steel chips, and large steel turnings), or 2.0 g (limestone, zeolite, and calcite) of adsorbent was added to a 250 mL Erlenmeyer flask containing 100 mL of 1.0-40.0 mg P/L solution. The solution was adjusted to pH 7.0 using 0.1 M NaOH. The flask was placed in a temperature controlled orbital shaker and was continuously shaken at 100 rpm for 24 h at 20 °C. After 24 h, the solution was filtered through a 0.45 μm filter and analyzed for P.

The equilibrium adsorption capacity, q_e (mg/g), was calculated by the following equation:

$$q_e = \frac{V\,(C_0 - C_e)}{m} \qquad \text{(Eq. 2.1)}$$

where C_0 and C_e are the initial and equilibrium liquid phase phosphorus concentrations (mg/L), respectively, V is the volume of the solution (L), and m is the mass of the adsorbent (g).

2.2.3 Adsorption Isotherms and Thermodynamics

Phosphorus adsorption isotherm experiments were conducted at three different temperatures (5, 20, and 30 °C). Langmuir and Freundlich isotherm models were used for fitting the experimental data. The Langmuir model assumes monolayer adsorption on a homogeneous surface while the Freundlich model assumes multilayer adsorption over a heterogeneous surface (Foo and Hameed 2010). The linearized form of the Langmuir model can be expressed mathematically as follows:

$$\frac{C_e}{q_e} = \frac{C_e}{q_{max}} + \frac{1}{K_L\, q_{max}} \quad \text{(Eq. 2.2)}$$

where q_{max} is the maximum adsorption capacity (mg/g) and K_L is the Langmuir constant (L/mg). The linearized form of the Freundlich model can be expressed mathematically as follows:

$$\ln q_e = \ln K_F + \frac{1}{n} \ln C_e \quad \text{(Eq. 2.3)}$$

where K_F and n are Freundlich constants indicative of the adsorption capacity and adsorption intensity, respectively. Thermodynamic parameters $\Delta G°$, $\Delta S°$, and $\Delta H°$ were calculated through the construction of an Arrhenius plot of ln $k°$ versus $1/T$ and are calculated as follows:

$$\Delta G° = -RT \ln k° \quad \text{(Eq. 2.4)}$$

$$\ln k° = \frac{\Delta S°}{R} - \frac{\Delta H°}{RT} \quad \text{(Eq. 2.5)}$$

where $\Delta G°$ is the Gibbs free energy change (kJ/mol), $\Delta S°$ is the entropy change (J/mol-K), $\Delta H°$ is the enthalpy change (kJ/mol), R is the universal gas constant (8.314 J/mol-K), T is the temperature (K), and $k°$ is the equilibrium constant.

2.2.4 Kinetics of Adsorption

Limestone, steel slag, medium steel chips, and small steel chips were chosen for further testing based on the results of the isotherm experiments. Phosphorus adsorption kinetics were evaluated at initial concentrations of 5.0 mg P/L (limestone) and 30.0 mg P/L (steel slag, medium steel chips, and small steel chips). Samples were collected at time intervals of 1 min, 5 min, 10 min, 30 min, 1 h, 3 h, 6 h, 12 h, and 24 h, filtered through a 0.45 μm filter, and analyzed for P. The adsorption data was fitted to pseudo first-order and pseudo second-order kinetic models.

The pseudo first-order kinetic model is as follows:

$$\log(q_e - q_t) = \log q_e - \frac{k_1 t}{2.303} \quad \text{(Eq. 2.6)}$$

where q_t is the adsorption capacity at time t (mg/g), t is the shaking time (h), and k_1 is the equilibrium rate constant of the pseudo first-order adsorption (h^{-1}). The pseudo second-order kinetic model is as follows:

$$\frac{t}{q_t} = \frac{1}{k_2 (q_e)^2} + \frac{1}{q_e} t \quad \text{(Eq. 2.7)}$$

where k_2 is the equilibrium rate constant of the pseudo second-order adsorption (g/mg-h).

2.2.5 pH Impact

The effect of pH on P adsorption was investigated using initial concentrations of 5.0 mg P/L (limestone) and 30.0 mg P/L (steel slag, medium steel chips, and small steel chips). Solutions were adjusted to initial pH values of 5.0, 6.0, 7.0 8.0, and 9.0 using 0.1 M HCl and 0.1 M NaOH and samples were collected after 24 h. The samples were filtered using a 0.45 μm filter and analyzed for P.

2.2.6 Nitrate, Sulfate, and DOC Impact

The effect of nitrate, sulfate, and two forms of DOC on the adsorption of P was investigated. Nitrate and sulfate stock solutions were prepared by dissolving potassium nitrate (KNO_3) and sodium sulfate anhydrous (Na_2SO_4) in deionized water, respectively. Samples were prepared with nitrate and sulfate concentrations of 0, 10.0, 20.0, and 50.0 mg NO_3^--N/L and 0, 100, 200, and 500 mg SO_4^{2-}/L in addition to 5.0 mg P/L (limestone) and 30.0 mg P/L (steel slag, medium steel chips, and small steel chips). Two forms of DOC, humic acid derived and woodchip leached, were added to the P solutions in concentrations of 0, 5.0, 20.0, and 50.0 mg DOC/L. Samples were taken after 24 h, filtered using a 0.45 μm filter, and analyzed for P. Humic acid stock solutions were prepared from a Suwannee River humic acid standard which was obtained from the International Humic Substances Society. Woodchip leached DOC was prepared by submerging washed playground woodchips in deionized water and decanting after seven days. The liquid was filtered through a 0.45 μm filter to remove any suspended solids present.

2.2.7 Desorption of P

To evaluate the desorption potential of the materials, solutions of 5.0 mg P/L (limestone) and 30.0 mg P/L (steel slag, medium steel chips, and small steel chips) were shaken for 24 h and analyzed for P. After the adsorption experiment, the adsorbents were carefully rinsed with deionized water. A 200 mL desorption solution containing 0.01 M KCl adjusted to pH 7.0 was added to the flask. The solution was shaken and samples were taken at 8 h, 1 d, 2 d, 4 d, and 10 d and analyzed for P.

2.2.8 Real Drainage Impact

Subsurface drainage water was collected from agricultural fields in Arlington, SD and Baltic, SD, both of which have installed denitrification woodchip bioreactors to convert nitrate into nitrogen gas at the end of the subsurface drainage line. The bioreactors feature control structures on the upstream and downstream ends. Drainage water was collected at both sites from the upstream end of the bioreactor, the downstream end of the bioreactor, and further downstream where the discharged drainage water enters a receiving stream. The real drainage samples were diluted to a 1:10 ratio with deionized water due to high calcium levels in the drainage water which formed Ca-P complexes without the presence of an adsorbent. Because of the tendency of small steel chips to form solid masses during the adsorption experiments, three mixing ratios of limestone and small steel chips were tested (10% steel, 20% steel, and 40% steel) along with steel slag and medium steel chips. The diluted drainage sample was spiked with P to 30 mg P/L. Samples were shaken for 24 h, filtered through a 0.45 μm filter, and analyzed for P.

2.2.9 Analytical Methods

Phosphate, nitrate, and sulfate concentrations were determined using a DX-500 ion chromatography system (Dionex, Sunnyvale, CA) equipped with a conductivity detector (CD-20, Dionex). Each sample was filtered through a 0.45 μm filter before the analysis. The pH of each solution was measured with an Orion 290A+ advanced ISE/pH/mV/OPR meter (Thermo Electron, Waltham, MA). The DOC concentrations were determined with a Shimadzu TOC-5000 Analyzer (Shimadzu Corp., Kyoto, Japan). All the batch adsorption experiments were conducted in duplicate except for the

isotherm and kinetics experiments. The results of the duplicate experiments are expressed with the average values and standard deviations.

2.3 Results and Discussion

2.3.1 Adsorption Isotherms and Thermodynamics

The P adsorption data for the eight materials was fitted to Langmuir and Freundlich isotherm models and the results are shown in Table 2.2. Although the natural minerals had high correlation coefficients (R^2) using the Freundlich model, all eight adsorption materials fit the Langmuir model well ($R^2 > 0.985$) at 20 °C, suggesting that the adsorption of P was characterized by the formation a monolayer of P molecules along the surface of the adsorbents. Graphically, the results of the P adsorption experiments fitted to the Langmuir isotherm model are shown in Figure 2.1 (a) and Figure 2.1 (b) for the natural minerals and the industrial byproducts, respectively. The Langmuir isotherm is characterized by a plateau where the adsorbent has reached saturation and all possible adsorption sites are occupied. At P equilibrium concentrations less than 3 mg/L, limestone and calcite showed the typical Langmuir shape. However, at P equilibrium concentrations greater than 3 mg/L, both materials experienced an increase in P removal, suggesting that another mechanism, such as surface precipitation, may be occurring. Similar behavior has been reported by other authors researching $CaCO_3$ based materials (Griffin and Jurinak 1973; Perassi and Borgnino 2014). Because of this, only the initial section of adsorption data was fitted to the Langmuir model for limestone and calcite.

The adsorption capacities of limestone, zeolite, and calcite were relatively similar to one another, ranging from 0.10 to 0.13 mg/g at 20 °C. Compared to the three natural

minerals, the industrial byproducts had adsorption capacities over one order of magnitude higher at 20 °C, ranging from 1.68 to 4.95 mg/g. Of the five industrial byproducts tested, iron filings and small steel chips had the highest adsorption capacities at 4.95 and 4.47 mg/g, respectively. However, both materials had a tendency to clump and form masses, thus raising concerns for potential clogging issues if used individually in field-scale agricultural subsurface drainage treatment. Steel slag has been evaluated for P removal by many authors in batch conditions (Agyei et al. 2002; Drizo et al. 2002; Oguz 2004; Xue et al. 2009). Drizo et al. (2002) reported adsorption capacities of steel slag ranging from 0.31 to 3.93 mg/g using different initial P concentration ranges, similar to the results found in this experiment. Compared to the steel slag, medium steel chips had a 38% greater adsorption capacity at a similar particle size with capacities of 1.68 and 2.70 mg/g, respectively. In previous work, Allred and Racharaks (2014) tested multiple Fe-based adsorption materials including a manufactured iron oxides/hydroxides product, a material relatively similar to the iron oxides on the surface of the steel byproducts tested in this study. The iron oxides/hydroxides material yielded a P adsorption capacity of 7.92 mg/g, higher than the capacities found in this experiment (2.54-4.47 mg/g). Additionally, Fu et al. (2013) found goethite, a stable iron oxide, to have an adsorption capacity of 4.43 mg/g under batch conditions, similar to the capacities found in this experiment. Between the three sizes of steel byproducts tested, small steel chips had an adsorption capacity 43% higher than the large steel turnings. The increase of P adsorption is likely due to the increase in surface area and possible adsorption sites at smaller particle sizes, which agrees with results found in other studies (Cucarella and Renman 2009; Lyngsie et al. 2014; Vohla et al. 2011). As a material that is typically wasted or recycled, steel

byproducts offer a high P adsorption capacity, making it a potentially promising adsorbent for field-scale subsurface drainage treatment.

The effect of temperature on the adsorption of P by medium steel chips and steel slag is illustrated in Figure 2.1 (c) and Figure 2.1 (d), respectively. P adsorption capacities and thermodynamic parameters for all materials tested are shown in Table 2.2. For all eight materials, the adsorption capacities increased by factors of 1.2 to 2.8 as the shaking temperature increased from 5 °C to 30 °C, indicating that P adsorption is more favorable at higher temperatures. The three steel byproducts increased by 41-46% in P adsorption capacity with the increase in temperature. A similar trend was noted for P removal using steel slag and iron-hydroxide eggshell waste (Agyei et al. 2002; Mezenner and Bensmaili 2009). In subsurface drainage, water temperature will be dependent on location and season. Therefore, a field-scale subsurface drainage treatment structure will more than likely have higher P removal efficiencies during the summer months and lower efficiencies in the cooler months. Thermodynamic parameters ($\Delta G°$, $\Delta H°$, and $\Delta S°$) were calculated using the obtained experimental data at 5, 20, and 30 °C. As temperature increased, all of the eight materials experienced an increase in negativity for Gibb's free energy change ($\Delta G°$) values, suggesting that the reaction becomes more spontaneous as temperature increases (Saha and Chowdhury 2011). All of the materials exhibited positive enthalpy change ($\Delta H°$) values, implying that the P adsorption reaction was endothermic. The $\Delta H°$ values can also give some insight on the mechanisms of P removal. Although no definite value for distinguishing sorption exists, low $\Delta H°$ values are typically associated with physical sorption, while high $\Delta H°$ values are associated with chemical sorption, such as ligand exchange (Loganathan et al. 2014). The $\Delta H°$ values of

iron filings and steel byproducts (63.4-105 kJ/mol) were much higher than natural minerals and steel slag (7.12-16.5 kJ/mol), indicating that natural minerals and steel slag may have undergone physical sorption while the iron-based materials experienced chemical sorption mechanisms. Entropy change (ΔS°) refers to the randomness at the solid/solution interface. The positive ΔS° values calculated suggest that there is an increase in randomness for all eight adsorbents as temperature increases.

2.3.2 Adsorption Kinetics

The rate of P adsorption onto the materials is shown in Figure 2.2. In general, all four of the selected materials exhibited fast adsorption kinetics. Small steel chips and medium steel chips reached 67% and 52% of the 24 h adsorption capacity within 6 h, respectively. In previous work, Zeng et al. (2004) found that iron oxide tailings adsorbed 71% of the 24 h capacity within 30 min. Limestone had very fast adsorption kinetics, reaching 98% of the 24 h adsorption capacity within 10 min. Karageorgiou et al. (2007) observed similar behavior for the adsorption of P onto calcite as 88 to 95% of the total adsorption occurred within 15 min. The parameters from fitting the adsorption data to pseudo first-order and pseudo second-order kinetic models are shown in Table 2.3. The adsorption data fits both models reasonably well ($R^2 \geq 0.962$) with the exception of medium steel chips for the pseudo second-order model ($R^2 = 0.933$). The predicted adsorption capacities from the pseudo second-order kinetic model are much closer to the capacities predicted by the Langmuir isotherm model. Because the pseudo second-order kinetic model and the Langmuir isotherm model both assume a monolayer adsorption process, the four materials more than likely follow second-order kinetics.

2.3.3 Effect of pH

Figure 2.3 shows the effect of pH on the adsorption of P onto the adsorbents. Depending on the soil type, subsurface drainage water has pH values that are slightly basic or acidic (Fausey et al. 1995; Rozemeijer et al. 2010). A pH range of 5.0-9.0 was selected for this study in order to investigate the P adsorption performance of the materials under a wide range of pH circumstances. The adsorption capacities of small steel chips and medium steel chips increased by 35% and 40%, respectively, from pH 9.0 to pH 5.0. Although P adsorption increased in steel slag between pH 7.0 and pH 5.0, it also increased between pH 7.0 and pH 9.0, indicating that there may be more than one mechanism occurring in the pH range. It has commonly been reported that P removal decreases at higher pH values due to an increase in negativity on the adsorbent surface as well as an increased concentration of OH^- competing with P for adsorption sites (Agyei et al. 2002; Fu et al. 2013; Xue et al. 2009). Limestone showed little to no impact on P adsorption over the pH range. Overall, the steel byproducts still showed high P adsorption capacities over the tested pH range, especially for typical subsurface drainage pH conditions.

2.3.4 Effect of Coexisting Substances

The effect of coexisting concentrations of nitrate and sulfate on the adsorption of P is shown in Figure 2.4 (a) and Figure 2.4 (b), respectively. Agricultural subsurface drainage typically contains moderate to high levels of nitrate and sulfate, based on fertilizer application and soil conditions (Fausey et al. 1995; Lawlor et al. 2008; Warneke et al. 2011). In this study, none of the four adsorbents were affected by the presence of nitrate or sulfate, even at high levels (NO_3^--N = 50.0 mg/L and SO_4^{2-} = 500 mg/L).

Previous studies using iron oxide based adsorbents have also reported limited to no impact on P adsorption by the presence of the two anions (Lalley et al. 2016; Weng et al. 2012). The results indicate that the materials tested have a higher affinity for P adsorption compared to the coexisting anions, suggesting that it is more difficult for nitrate and sulfate ions to compete for adsorption sites.

The effect of coexisting concentrations of humic acid derived DOC and woodchip leached DOC on the adsorption of P is shown Figure 2.5 (a) and Figure 2.5 (b), respectively. Woodchip denitrification bioreactors have the potential to leach high levels of DOC, especially in the initial startup phase (Cameron and Schipper 2010; Warneke et al. 2011). All four materials were affected by the presence of both forms of DOC, especially at high concentrations. In the presence of 50.0 mg/L humic acid derived DOC, the P adsorption capacities of limestone, steel slag, medium steel chips, and small steel chips were reduced by 34%, 47%, 23%, and 10%, respectively. Similarly, 50.0 mg/L woodchip leached DOC reduced P adsorption capacities by 34%, 33%, 24%, and 17%, respectively. Both forms of DOC had a similar influence on the materials. Fu et al. (2013) found a reduction in P adsorption of 28% onto the iron oxide goethite with the addition of soil-derived humic acid. Weng et al. (2012) saw an even larger impact as the presence of DOC decreased P adsorption onto iron oxides by 37 to 97%. As the inhibition of P adsorption tended to increases with higher DOC concentrations, competitive adsorption of DOC and P onto the materials is likely the main mechanism. Although steel byproducts still adsorb large amounts of P in the presence of DOC, it is recommended that woodchip denitrification bioreactors are flushed before steel media installation to prevent DOC accumulation on adsorption sites.

2.3.5 Desorbability of P

The desorbability of P over time is shown in Figure 2.6. After an initial batch adsorption test to load the materials with P, another batch test was performed using a pH 7.0, 0.01 M KCl electrolyte solution to examine whether the materials would desorb under typical subsurface drainage conditions. The ability for materials to retain previously adsorbed P is critical to the success of field-scale application as the release of P will increase the nutrient loading to natural water bodies. Over a period of 10 d, limestone and steel slag desorbed 9.6 and 0.6% of the attached P, respectively. Neither of the steel byproducts released any P over the 10 d period. In a study that tested four iron-based adsorbents, Allred and Racharaks (2014) found that 0 to 3% of the adsorbed P was desorbed during a deionized water wash. When a K_2SO_4 electrolyte was used, still only 0 to 7% of the adsorbed P was desorbed. It is possible that the desorbability of the adsorbents is directly related to the ΔH° values found in this study. As previously noted, ΔH° can be an indication of whether the material undergoes physical sorption (low ΔH°) or chemical sorption (high ΔH°) as its primary mechanism. Limestone and steel slag both had somewhat low ΔH° values. Since physical sorption involves relatively weak electrostatic interactions, limestone and steel slag may have been more prone to releasing P back into the solution. On the other hand, the strong chemical bonds formed between the steel byproducts and P make them less susceptible to releasing P. However, there is still potential to recover the P and possibly recharge the adsorbents. High concentration NaOH solutions have been used previously to desorb the P (Genz et al. 2004; Lalley et al. 2016; Nguyen et al. 2015). Although additional research is needed to analyze the

desorption potential of steel byproducts, it may be possible to extend the lifespan of a field-scale subsurface drainage treatment system using this technique.

2.3.6 Real Drainage Impact

The effect of subsurface and surface drainage matrixes from Arlington, SD and Baltic, SD on the adsorption of P are shown in Figure 2.7 (a) and Figure 2.7 (b), respectively. Because of the tendency for small steel chips to form masses, three mixing ratios with limestone were tested for a more realistic subsurface drainage treatment media. The mixing ratios of 10% steel, 20% steel, and 40% steel yielded adsorption capacities of 0.95, 1.42, and 2.28 mg/g, respectively. The results show that even while mixing the small steel chips with another media, they can still adsorb P at a relatively high level. The drainage matrixes from the Arlington site did not have a noticeable trend in terms of effect on the P adsorption capacities of the adsorbents. Generally, the adsorbents still exhibited high adsorption capacities. The matrixes collected from the Baltic site had more of an impact on P adsorption, especially the downstream sample. The Baltic downstream matrix reduced P adsorption capacities by 24 to 48% between the adsorbents tested. This may have been a result of higher DOC concentrations in the matrix, competing for adsorption sites and decreasing the P adsorption capacities. Although adsorption capacities are reduced, the steel byproducts still showed high P removal potential in real drainage matrixes.

2.3.7 Material Selection and Field-Scale Installation

The results of the batch experiments indicate that the carbon steel byproducts tested have high potential to remove P and can be used for full-scale agricultural subsurface drainage treatment. Steel byproducts are also very inexpensive, with prices

ranging from $0.02 to 0.03/lb when collected from local machine shops. Because of their P removal efficiency and low cost, the steel byproducts were placed in an 8’ long, 18” diameter non-perforated subsurface drainage cartridge and installed at the Baltic, SD site following the existing denitrification woodchip bioreactor. Continuous monitoring of P removal performance will take place until the steel byproducts are exhausted. In addition to monitoring the field-scale subsurface treatment system, column testing is recommended to further understand the dynamics of P adsorption onto steel byproducts. Continuous flow-through column testing provides experimental conditions similar to field-scale conditions, allowing for more accurate predictions of performance and longevity.

2.4 Conclusions

Three natural minerals and five industrial byproducts were tested for P adsorption under various conditions in order to determine their potential for treating agricultural subsurface drainage. The materials tested all fit the Langmuir isotherm model, which indicated that the adsorption of P was monolayer across the adsorbents’ surfaces. Industrial byproducts exhibited substantially higher adsorption capacities than natural minerals, ranging from 1.68 to 4.95 mg/g compared to 0.10 to 0.13 mg/g at 20 °C. The three sizes of steel byproducts exhibited P adsorption capacities of 2.54 to 4.47 mg/g, which were comparable to steel slag and the iron filings. Increasing temperature had a large impact on the adsorption of P, as adsorption capacities were 1.2 to 2.8 times higher at 30 °C than 5 °C. The steel byproducts exhibited relatively fast kinetics, as 60% of the adsorption took place in 8 h. Decreasing pH resulted in an increase in adsorption among

the steel byproducts. The presence of varying concentrations of coexisting anions nitrate and sulfate had little impact on P removal. However, increasing concentrations of DOC inhibited P adsorption by up to 24% for steel byproducts. While limestone desorbed 9% over 10 h, the strong chemical bonds between P and steel byproducts prevented the release of P. Steel byproducts were able to effectively adsorb P from spiked real drainage samples. Overall, the results of this study suggest that steel byproducts are highly efficient adsorption materials that potentially can be used as filter media for P removal from agricultural subsurface drainage.

Table 2.1: Characteristics of natural minerals and industrial byproducts.

Material	Size[a] (mm)	Particle Density (g/cm^3)	pH[b]	Moisture Content	Organic Content
Limestone	0.9-2.0	2.76	8.3	0%	0.4%
Zeolite	0.9-2.0	2.18	8.0	3.2%	4.7%
Calcite	0.9-2.0	2.64	8.4	0%	0.8%
Steel Slag	0.9-4.8	3.57	10.9	0.7%	2.0%
Iron Filings	0.1-2.0	5.91	6.5	0%	0%
Small Steel Chips	0.1-2.0	5.20	6.3	0%	0%
Medium Steel Chips	2.0-4.8	5.50	6.3	0%	0%
Large Steel Turnings	10-30	5.54	6.3	0%	0%

[a] Size ranges determined from known sieve sizes except for large steel turnings, which were measured manually.

[b] Values of pH were obtained from a 1:1 by weight slurry mixture of material and distilled water.

Table 2.2: Langmuir and Freundlich isotherm constants and thermodynamic parameters for the adsorption of P onto natural minerals and industrial byproducts.

Material	Temp. (°C)	Langmuir Isotherm			Freundlich Isotherm			Thermodynamics		
		q_{max} (mg/g)	K_L (L/mg)	R^2	K_F	n	R^2	ΔG° (kJ/mol)	ΔH° (kJ/mol)	ΔS° (J/mol-K)
Limestone	5	0.10	0.87	0.992	0.05	2.80	0.871	0.32		
	20	0.11	0.94	0.985	0.05	2.25	0.991	0.15	7.12	24.2
	30	0.22	1.14	0.984	0.08	1.58	0.995	-0.33		
Zeolite	5	0.10	0.81	0.995	0.05	1.94	0.917	0.49		
	20	0.13	0.93	0.993	0.05	2.77	0.943	0.17	7.59	25.4
	30	0.17	1.07	0.998	0.08	2.89	0.854	-0.16		
Calcite	5	0.08	0.97	0.992	0.05	3.05	0.885	0.07		
	20	0.10	1.10	0.986	0.05	2.46	0.998	-0.24	10.2	36.3
	30	0.20	1.42	0.970	0.09	1.42	0.999	-0.88		
Steel Slag	5	0.97	1.01	0.982	0.55	6.15	0.763	-0.02		
	20	1.68	1.81	0.998	1.08	6.37	0.973	-1.44	29.3	105
	30	2.40	2.91	0.998	1.49	4.70	0.905	-2.69		
Iron Filings	5	4.57	1.01	0.990	2.55	5.01	0.912	-0.02		
	20	4.95	13.2	0.999	3.11	5.26	0.950	-6.29	84.8	306
	30	5.37	18.4	0.998	4.19	8.72	0.945	-7.34		
Small Steel Chips	5	3.12	1.02	0.959	2.44	24.0	0.586	-0.05		
	20	4.47	9.44	0.999	3.46	7.96	0.943	-5.47	92.8	334
	30	5.33	27.2	0.999	4.56	10.6	0.672	-8.32		
Medium Steel Chips	5	1.97	1.07	0.999	1.09	4.62	0.940	-0.16		
	20	2.70	12.7	0.995	1.41	9.07	0.707	-6.19	105	377
	30	3.38	43.5	0.999	3.16	5.65	0.837	-9.51		
Large Steel Turnings	5	1.54	1.54	0.995	1.05	7.65	0.878	-1.01		
	20	2.54	4.81	0.998	1.92	10.3	0.913	-3.83	63.4	231
	30	2.88	15.5	0.999	2.36	7.87	0.870	-6.91		

*Experimental conditions: initial PO_4^{3-}-P=1.0-40.0 mg/L; pH=7.0; adsorption time=24 h.

Table 2.3: Kinetic parameters for the adsorption of P.

Material	$q_{e,\ Langmuir}$ (mg/g)	Pseudo first-order model			Pseudo second-order model		
		k_1 (h^{-1})	$q_{e,\ 1}$ (mg/g)	R^2	k_2 (g/mg-h)	$q_{e,\ 2}$ (mg/g)	R^2
Limestone	0.11	1.44	0.04	0.962	1050	0.09	0.998
Steel Slag	1.68	0.21	1.03	0.969	0.71	1.61	0.989
Medium Steel Chips	2.70	0.17	2.26	0.993	0.18	2.45	0.933
Small Steel Chips	4.47	0.14	3.55	0.989	0.13	4.74	0.975

*Experimental conditions: initial PO_4^{3-}-P=30.0 mg/L and 5.0 mg/L (limestone); temperature=20 °C; pH=7.0.

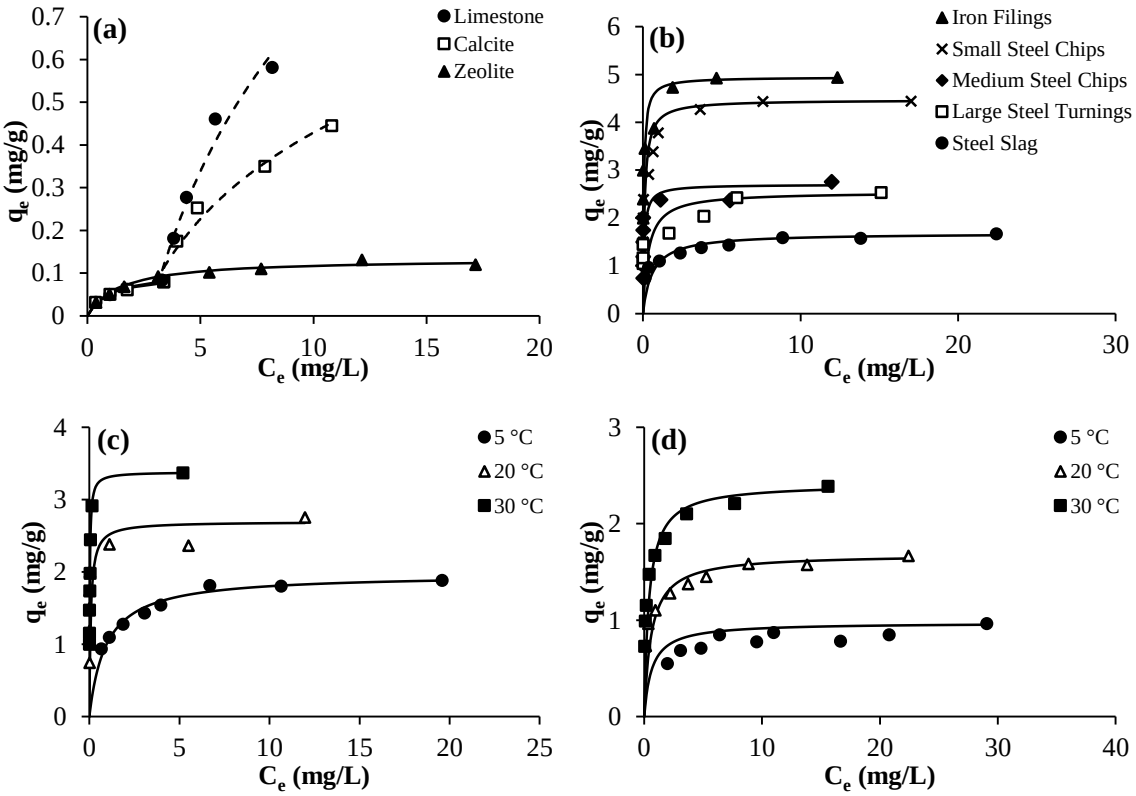

Figure 2.1: Langmuir adsorption isotherms. (Experimental conditions: initial PO_4^{3-}-P=1.0-40.0 mg/L; pH=7.0; adsorption time=24 h. (a) Natural minerals. (b) Industrial byproducts. (c) Effect of temperature on medium steel chips. (d) Effect of temperature on steel slag.)

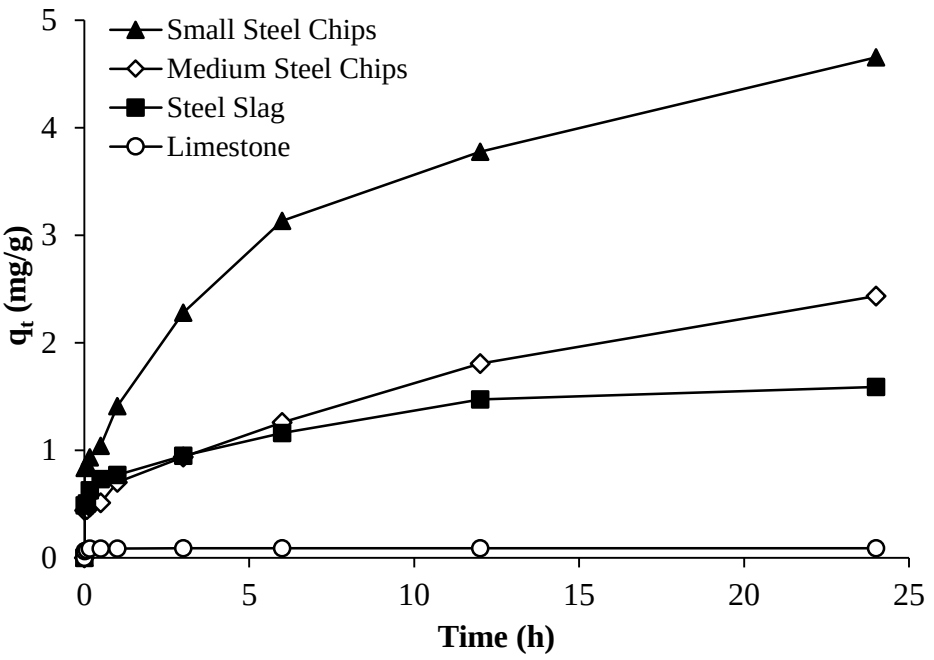

Figure 2.2: Effect of time on P adsorption. (Experimental conditions: initial PO_4^{3-}-P=30.0 mg/L and 5.0 mg/L (limestone); temperature=20 ℃; pH=7.0.)

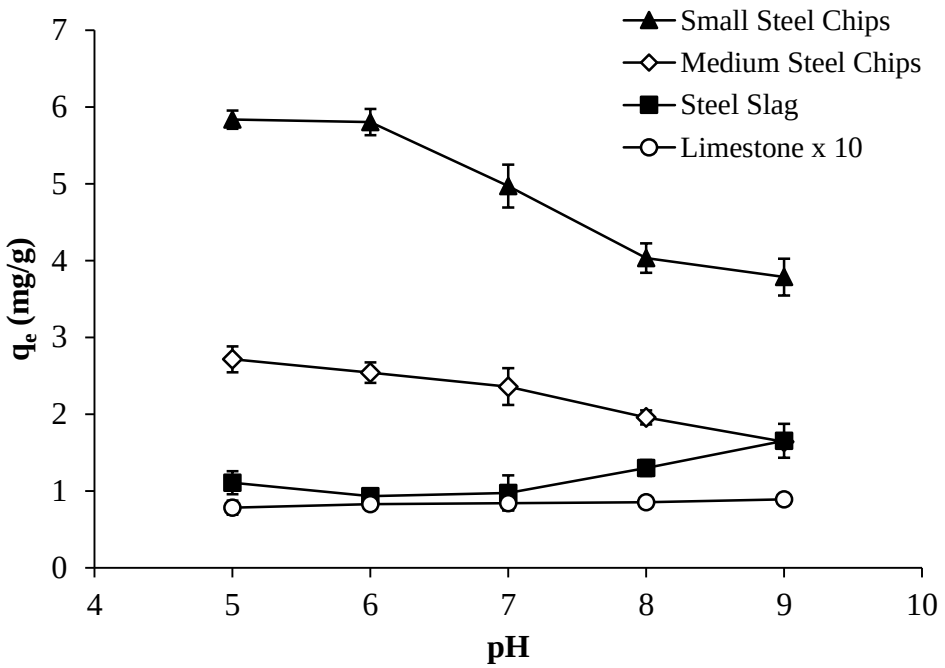

Figure 2.3: Effect of pH on P adsorption. (Experimental conditions: initial PO_4^{3-}-P=30.0 mg/L and 5.0 mg/L (limestone); temperature=20 °C; adsorption time=24 h; error bars indicate standard deviation.)

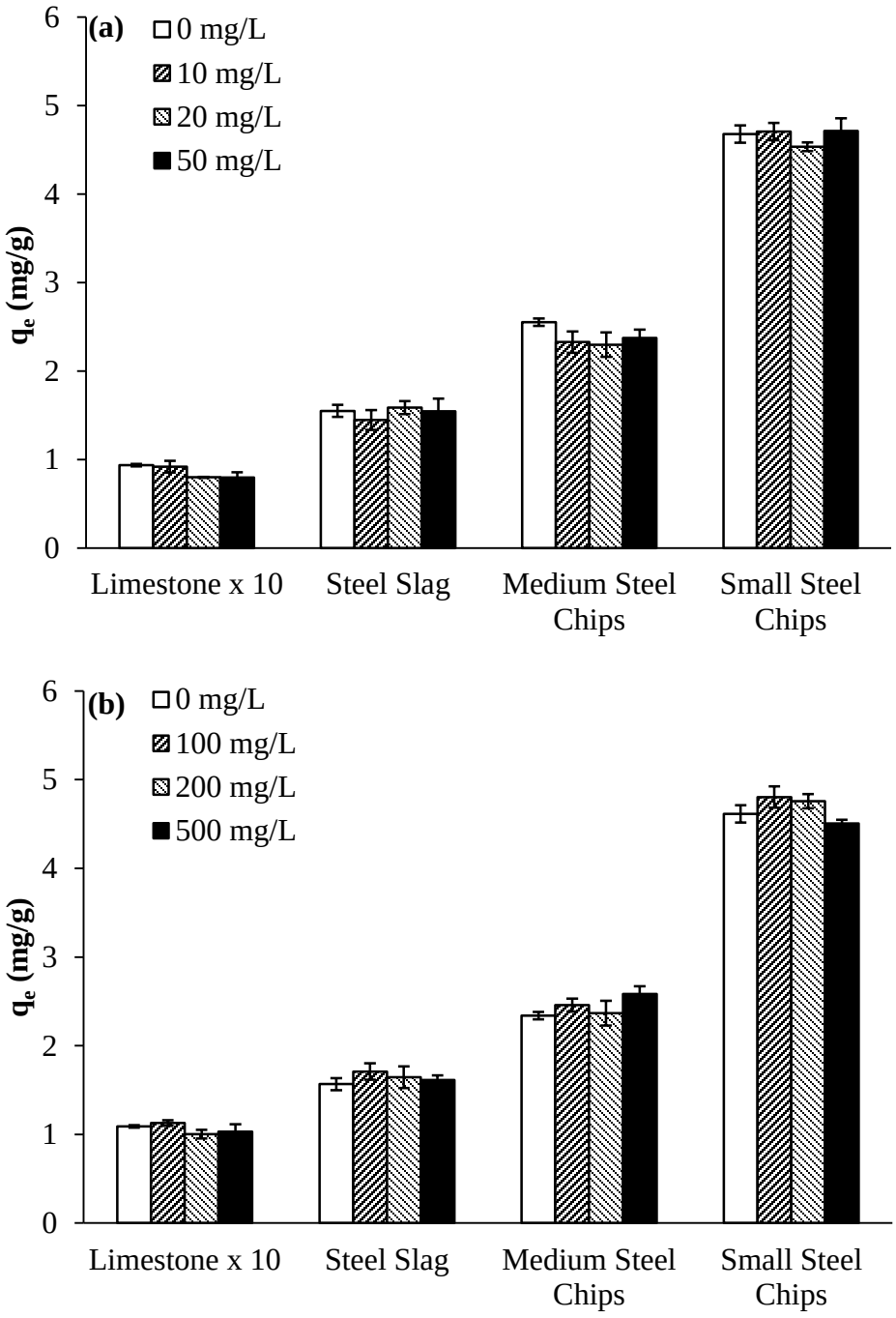

Figure 2.4: Effect of coexisting anions on P adsorption. (Experimental conditions: initial PO_4^{3-}-P=30.0 mg/L and 5.0 mg/L (limestone); temperature=20 °C; pH=7.0; adsorption time=24 h; error bars indicate standard deviation. (a) NO_3^--N=0-50.0 mg/L. (b) SO_4^{2-}=0-500 mg/L.)

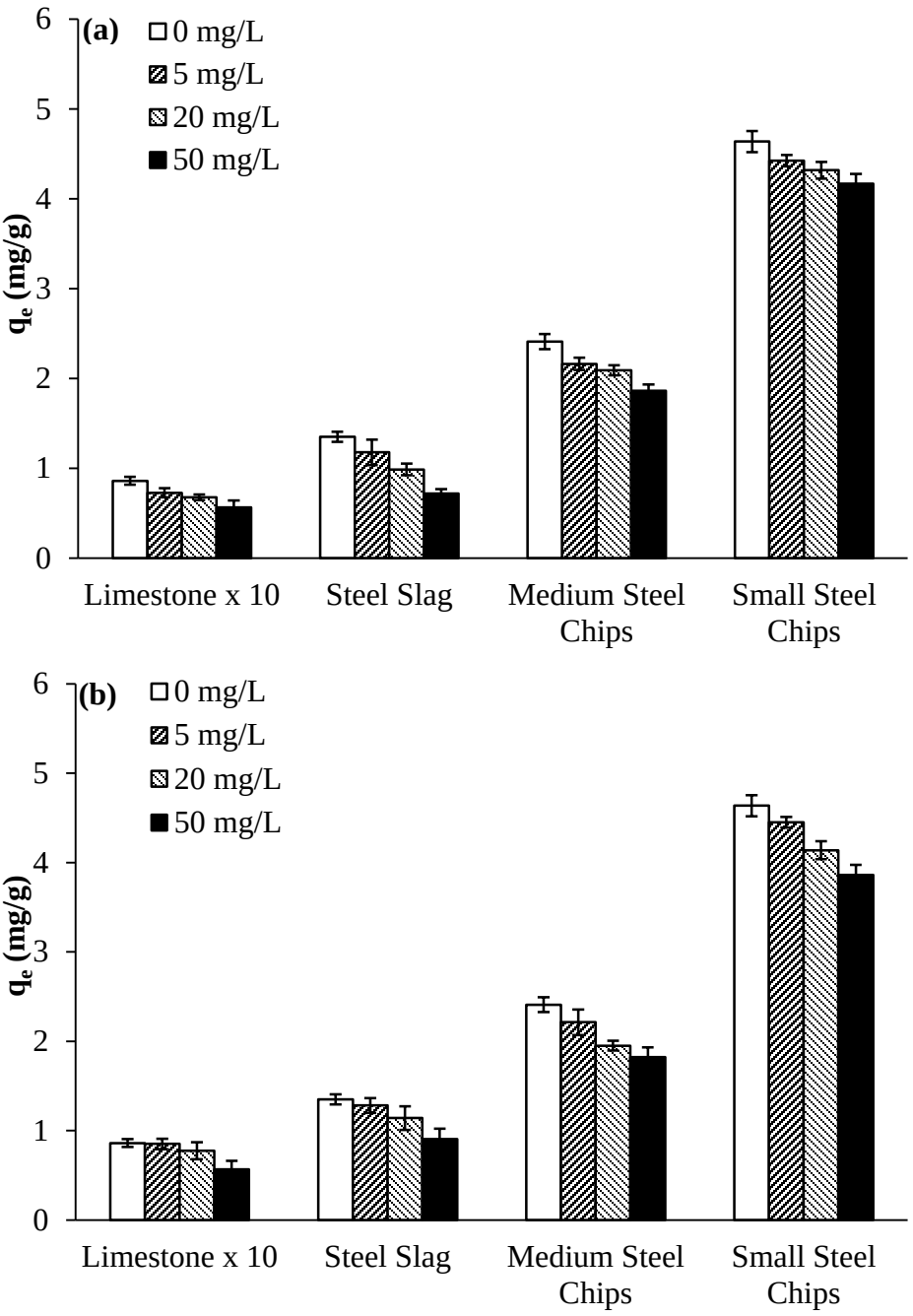

Figure 2.5: Effect of DOC on P adsorption. (Experimental conditions: initial PO_4^{3-}-P=30.0 mg/L and 5.0 mg/L (limestone); temperature=20 °C; pH=7.0; adsorption time=24 h; error bars indicate standard deviation. (a) Humic acid derived DOC=0-50.0 mg/L. (b) Woodchip leached DOC=0-50.0 mg/L.)

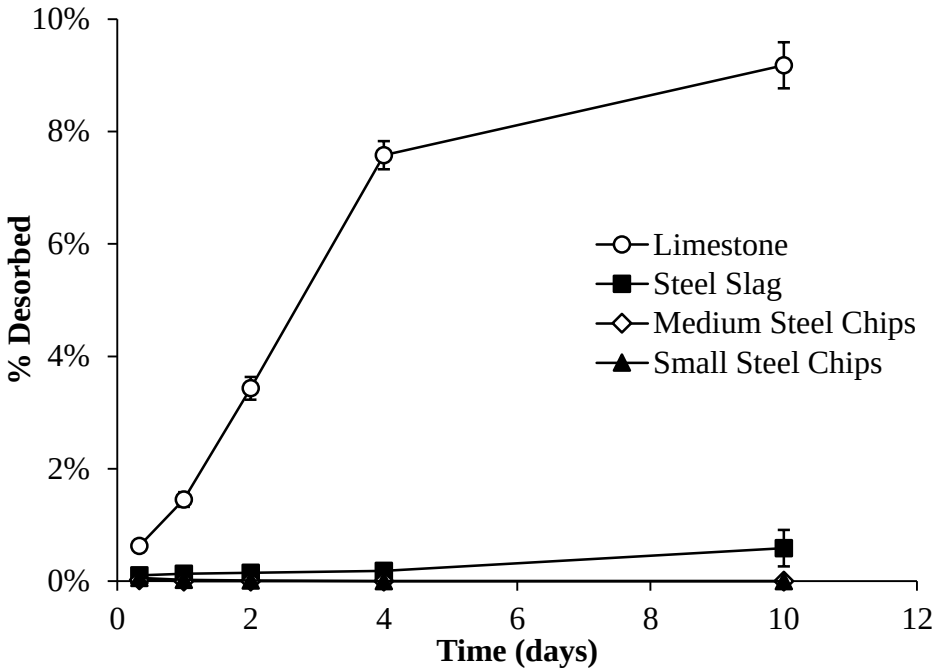

Figure 2.6: Desorption of P. (Experimental conditions: desorption time=0-10 d, temperature=20 °C; pH=7.0; error bars indicate standard deviation.)

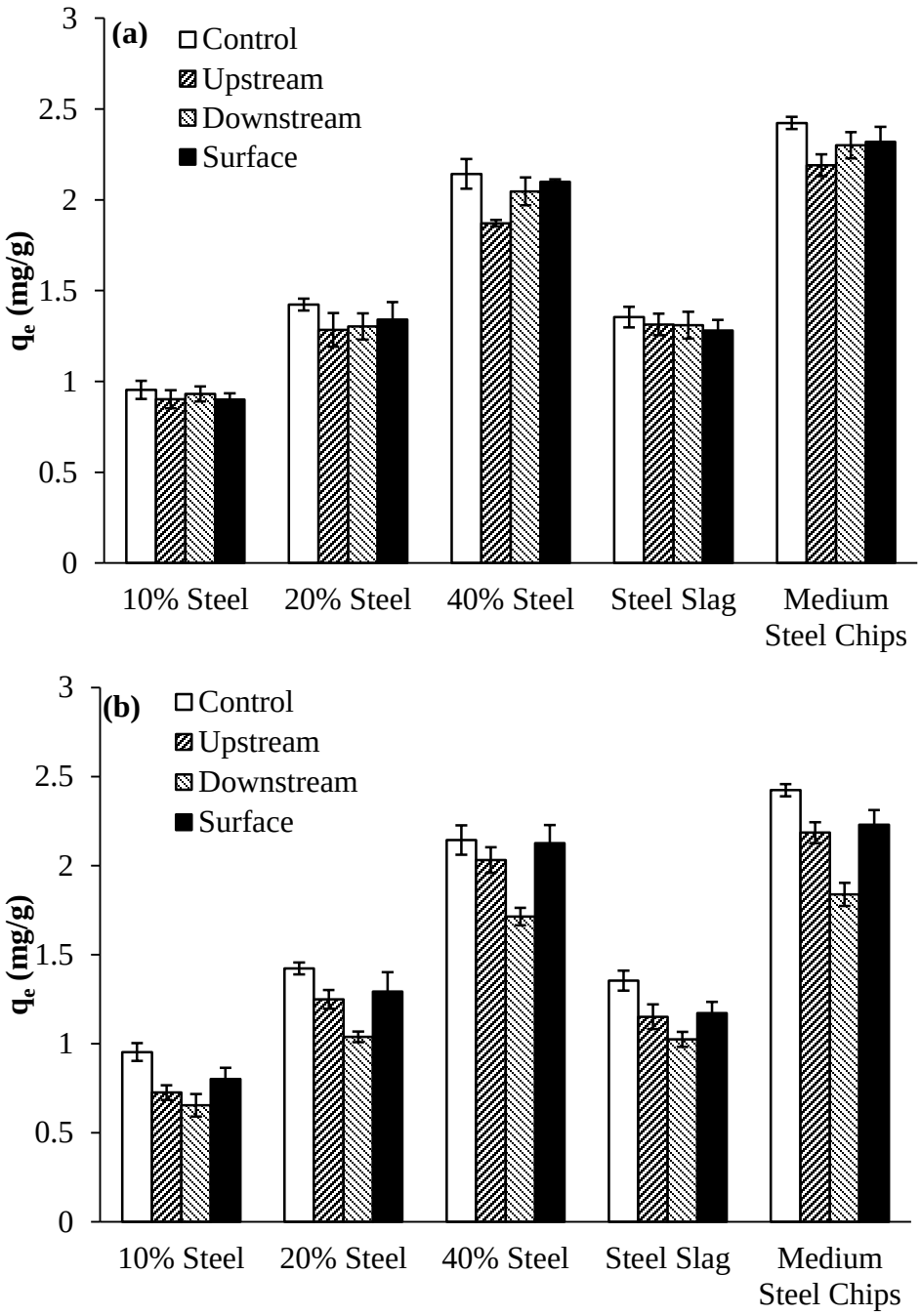

Figure 2.7: Effect of spiked drainage water matrixes on P adsorption. (Experimental conditions: initial PO_4^{3-}-P=30.0 mg/L; temperature=20 °C; pH=7.0; adsorption time=24 h; error bars indicate standard deviation. (a) Arlington, SD. (b) Baltic, SD.)

CHAPTER 3

ADSORPTION OF PHOSPHATE USING STEEL BYPRODUCTS TO TREAT AGRICULTURAL SUBSURFACE DRAINAGE: A FIXED-BED COLUMN STUDY

3.1 Introduction

The installation of subsurface or "tile" drainage has become a common agricultural practice in the Midwestern United States, Canada, and other areas with poorly drained soils (Fausey et al. 1995; King et al. 2015). Composed of a network of perforated pipes buried underneath the soil, subsurface drainage systems remove excess water from the soil profile, increasing and providing more uniform crop production (Zucker and Brown 1998). While it is necessary to make agricultural production possible in many areas, the addition of subsurface drainage can also increase crop yields by 5 to 25% (Eidman 1997). However, the increase in water infiltration facilitates the transport of soil-applied nutrients to subsurface drains, which provide a direct pathway for nutrients to nearby water bodies (Fausey et al. 1995; King et al. 2015). Excess nutrient loading on surface waters can lead to eutrophication, resulting in algal blooms, anoxia, and fish kills (Correll 1998).

Phosphorus (P) is typically the limiting nutrient in freshwater ecosystems, with total P concentrations $\geq$ 0.02 mg/L a concern for the development of eutrophic conditions (Correll 1998; Heathwaite and Dils 2000). Surface runoff and subsurface flow are the two main mechanisms for P loss from agricultural soils. Historically, surface runoff has been recognized as the primary mechanism for P transport from agricultural fields to surface water bodies (Baker et al. 1975; Sharpley et al. 1994). However, recent studies have established that P loss via subsurface drainage is substantial, especially in locations with high soil P levels and soils with low P sorption capacities (Sims et al. 1998). Additionally,

P losses in subsurface drainage are typically dominated by dissolved P, which is immediately available for rapid biological uptake (Algoazany et al. 2007; Hansen et al. 2002). In a study by King et al. (2015), the authors measured discharge data over an eight-year span from six tile drains in a watershed in central Ohio and found that greater than 90% of the water samples collected exceeded the 0.02 mg/L threshold, with dissolved P concentrations reaching as high as 4.64 mg/L. In another study, Gentry et al. (2007) found average dissolved P concentrations ranging from 0.03-0.31 mg/L over a two-year period for three tile drains in east-central Illinois.

To prevent further damage to surface water ecosystems, it is crucial to develop strategies to treat agricultural subsurface drainage. Adsorption has emerged as a promising P removal technique due to its effectiveness, ease of operation, low-cost, and P recovery potential (Onyango et al. 2007). In previous batch and column studies, various forms of natural minerals, industrial byproducts, and synthetic products such as limestone, zeolite, steel slag, iron oxides, drinking water treatment residual, and granular activated carbon have been used to remove P (Allred and Racharaks 2014; Chardon et al. 2012; Drizo et al. 2002; Grace et al. 2015; Lyngsie et al. 2014; Reddy et al. 2014). These materials are typically rich in calcium (Ca), aluminum (Al), and iron (Fe) where Ca-based materials have a tendency to form Ca-P precipitates while Al/Fe-based materials can precipitate and adsorb P (Penn et al. 2011; Stoner et al. 2012). Researchers have used these materials to build reactive filters/barriers for P removal from storm water runoff, poultry farm runoff, and tile-drained land (Erickson et al. 2012; McDowell et al. 2008; Penn et al. 2014). Batch and column studies have been used to predict the performance of such P removal structures. However, column studies are recognized as a more suitable approach due to their ability to

simulate constant flow-through P application and realistic retention times (Drizo et al. 2002; Penn and McGrath 2011; Stoner et al. 2012).

Steel byproducts are a promising new Fe-based material that is readily available in many areas, inexpensive, and has high P removal potential. Composed of several sizes of chips and turnings, steel byproducts oxidize in the presence of water and oxygen, continuously forming reactive layers of Fe oxides that are potential adsorption sites for P. Previous work has investigated specially developed and manufactured Fe-based products such as iron filings, zero-valent iron, and other forms of modified iron oxides, yielding high adsorption capacities (Allred and Racharaks 2014; Lalley et al. 2016; Reddy et al. 2014). As a material that is typically landfilled or recycled back into the steel making industry, steel byproducts potentially offer a low-cost solution for P removal from agricultural subsurface drainage.

The objective of this study was to evaluate the P adsorption capabilities of steel byproducts in a flow-through column and determine their potential for agricultural subsurface drainage treatment. An initial batch adsorption experiment was performed for comparison purposes. The effects of influent P concentration, empty bed contact time (EBCT), influent pH, presence of dissolved organic carbon (DOC) on P removal in a flow-through column were investigated. A mixed contaminant study was performed to examine the removal of P, nitrate, DOC, Cu, and Zn by steel byproducts. The desorbability of P was also investigated. To further quantify P adsorption onto steel byproducts, steel slag was tested as a reference material.

3.2 Materials and Methods

3.2.1 Adsorbents

Carbon steel byproducts and electric arc furnace steel slag were evaluated in this study. The steel byproducts were collected from Prairie Manufacturing, LLC (Sioux Falls, SD), a machine shop that cuts, shapes, and finishes carbon steel. Large amounts of steel chips and turnings are produced as a byproduct, which are typically recycled or landfilled. The steel byproducts are graded as 1018 carbon steel. Electric arc furnace steel slag is a byproduct of the steel making industry produced by using an electric current to melt scrap metal and fluxes to a liquid state. The fluxes combine with the nonmetallic components forming a liquid slag, which is separated from the liquid steel and allowed to cool, producing the steel slag byproduct. The steel slag was collected from Nucor Corporation (Norfolk, NE).

The steel byproducts and steel slag were washed with deionized water to remove dirt and fine particles. To remove any oil on the surface, the steel byproducts were also washed with phosphate-free soap. Washed materials were air dried overnight. During the drying process, the steel byproducts oxidized, forming a layer of rust on the steel surface. After drying, the steel byproducts and steel slag were sieved to a desired size range and subjected to physical and chemical characterization tests. The physical and chemical properties of steel byproducts and steel slag are shown in Table 3.1. The steel byproducts were sieved and sorted to three different sizes: small steel chips (0.1-2.0 mm), medium steel chips (2.0-4.8 mm), and large steel chips (10-20 mm). For comparison purposes, steel slag was sieved to a similar size range as the medium steel chips (2.0-4.8 mm). Particle densities were calculated by measuring the volume of water displaced by a

known mass of material. The three sizes of steel byproducts had higher particle densities (5.20-5.54 g/cm^3) than the steel slag (3.57 g/cm^3), which is due to differing elemental makeup of the materials. The predominant species in steel byproducts is Fe, which has an elemental density of 7.87 g/cm^3, while steel slag contains Fe along with substantial amounts of Ca and Mg, which have elemental densities of 1.54 g/cm^3 and 1.74 g/cm^3, respectively (Drizo et al. 2002). The measurement of pH values was performed following ASTM D4972. Steel byproducts were slightly acidic (pH = 6.3), while steel slag was alkaline (pH = 10.9). Packing densities were calculated by dividing the occupied column volume from the amount of mass of material needed to reach the desired volume. Steel slag had the highest packing density of the tested materials (1.80 g/cm^3) while the packing density increased with decreasing particle size for the three sizes of steel byproducts (0.64-1.40 g/cm^3). Hydraulic conductivities were measured using the falling-head permeability method (ASTM D5084). The hydraulic conductivities of the steel byproducts increased with increasing particle size (0.31-3.24 cm/s) and steel slag had a hydraulic conductivity of 1.01 cm/s. All four materials exhibited hydraulic conductivities much greater than 1 x 10^{-3} cm/s, the lowest recommended hydraulic conductivity for sand filtration systems (Claytor and Schueler 1996).

3.2.2 Batch P Adsorption Experiment

Phosphorus stock solution was prepared by dissolving monopotassium phosphate (KH_2PO_4) in deionized water. For each experiment, 0.5 g (small steel chips) or 1.0 g (steel slag, medium steel chips, and large steel chips) of adsorbent was added to a 250 mL Erlenmeyer flask containing 100 mL of 10.0-40.0 mg P/L solution. The solution was adjusted to pH 7.0 using 0.1 M NaOH. The flask was placed in a temperature controlled

orbital shaker and was continuously shaken at 100 rpm for 24 h at 20 °C. After 24 h, the solution was filtered through a 0.45 μm filter and analyzed for P. The equilibrium adsorption capacity, q_e (mg/g), was calculated by the following equation:

$$q_e = \frac{V\,(C_0 - C_e)}{m} \quad \text{(Eq. 3.1)}$$

where C_0 and C_e are the initial and equilibrium liquid phase phosphorus concentrations (mg/L), respectively, V is the volume of the solution (L), and m is the mass of the adsorbent (g).

Langmuir and Freundlich isotherm models were used for fitting the experimental data. The Langmuir model assumes monolayer adsorption, with a finite number of adsorption sites on the material surface. Alternatively, the Freundlich model assumes multilayer adsorption over a heterogeneous surface (Foo and Hameed 2010). The linearized form of the Langmuir model can be expressed mathematically as follows:

$$\frac{C_e}{q_e} = \frac{C_e}{q_{max}} + \frac{1}{K_L\, q_{max}} \quad \text{(Eq. 3.2)}$$

where q_{max} is the maximum adsorption capacity (mg/g) and K_L is the Langmuir constant (L/mg).

The linearized form of the Freundlich model can be expressed mathematically as follows:

$$\ln q_e = \ln K_F + \frac{1}{n} \ln C_e \quad \text{(Eq. 3.3)}$$

where K_F and n are Freundlich constants indicative of the adsorption capacity and adsorption intensity, respectively.

3.2.3 Column P Adsorption Experiments

The column adsorption tests were conducted in Omnifit® fixed-bed glass columns of 15 cm height and 1.5 cm inner diameter. A known mass of small steel chips,

medium steel chips, large steel chips, and steel slag was packed into the columns to achieve a bed height of 10 cm. Solutions of varying P concentrations (1.0, 10.0, and 50.0 mg P/L), initial pH values (5.0, 7.0, and 9.0), and DOC concentrations (0, 5.0, and 25.0 mg DOC/L) were pumped from the bottom of the columns upward at flow rates of 17.7, 5.89, and 1.77 mL/min to achieve EBCTs of 1, 3, and 10 min using a peristaltic pump. Effluent samples were collected at definite time intervals for a duration of 4800 empty bed volumes (3.33, 10.0, or 33.3 d based upon EBCT), filtered through a 0.45 μm filter, and analyzed for P.

The empty bed contact time (EBCT) in the column is achieved from the ratio of bed volume (mL) to the volumetric flow rate, *Q* (mL/min), and is calculated as follows:

$$EBCT = \frac{Bed\ Volume}{Q} \quad \text{(Eq. 3.4)}$$

Breakthrough curves and cumulative P retained curves were constructed to show the adsorption behavior of P onto steel byproducts and steel slag. The breakthrough curves show the loading behavior of P onto the fixed-bed columns and are expressed as the ratio of inlet P concentration to outlet P concentration (C/C_0) as a function of time. Plotting cumulative P retained curves as a function of empty bed volumes can illustrate the performance and capacities of the adsorption media. For a given initial P concentration and flow rate, the total mass of P adsorbed, q_{total} (mg P), can be calculated as being equal to the area under the plot of the adsorbed P concentration versus time. Furthermore, the equilibrium P adsorption capacity of the material, q_e (mg/g), can be found by dividing q_{total} by the mass of material in the column. q_{total} and q_e are calculated as follows:

$$q_{total} = \frac{Q}{1000}\int_{t=0}^{t=total} C_{ad}\,dt \quad \text{(Eq. 3.5)}$$

$$q_e = \frac{q_{total}}{m} \quad \text{(Eq. 3.6)}$$

where C_{ad} is the concentration of adsorbed P ($C_{ad} = C_0 - C$) (mg/L) and t is time (min).

3.2.4 Desorption of P

To evaluate the desorbability and recovery of P from exhausted medium steel chips, four desorption solutions were used and compared including 0.01 M KCl, 0.05 M NaOH, 0.10 M NaOH, and 0.20 M NaOH. Columns were initially loaded with P by pumping a 10.0 mg P/L solution adjusted to pH 7.0 at a flow rate of 17.7 mL/min (EBCT = 1 min) for 4800 empty bed volumes (3.33 days). Prior to desorption, P loaded columns were rinsed with distilled water at a flow rate of 5.89 mL/min for 15 min. The desorption solutions were passed through the columns at a flow rate of 5.89 mL/min (EBCT = 3 min) for 120 empty bed volumes (6.0 h). Effluent samples were collected at definite time intervals, filtered through a 0.45 μm filter, and analyzed for P.

3.2.5 Mixed Contaminant Removal

Medium steel chips were used to evaluate the removal of several possible agricultural subsurface drainage contaminants including phosphate (PO_4^{3-}-P), nitrate (NO_3^--N), DOC, copper (Cu), and zinc (Zn) simultaneously in a fixed-bed column. Stock solutions were prepared using monopotassium phosphate (KH_2PO_4), potassium nitrate (KNO_3), woodchip leached DOC, copper sulfate pentahydrate ($CuSO_4 \cdot 5H_2O$), and zinc sulfate heptahydrate ($ZnSO_4 \cdot 7H_2O$). An influent solution of 1.0 mg PO_4^{3-}-P/L, 10.0 mg NO_3^--N /L, 5.0 mg DOC/L, 0.5 mg Cu/L, and 0.5 mg Zn/L adjusted to pH 7.0 was pumped upward through the column at a flow rate of 5.89 mL/min (EBCT = 3 min) for a total of 4800 empty bed volumes (10 d). Effluent samples were collected at definite time intervals, filtered through a 0.45 μm filter, and analyzed for all constituents.

3.2.6 Analytical Methods

Phosphate and nitrate concentrations were determined using a DX-500 ion chromatography system (Dionex, Sunnyvale, CA) equipped with a conductivity detector (CD-20, Dionex). The pH of solutions was measured with an Orion 290A+ advanced ISE/pH/mV/OPR meter (Thermo Electron, Waltham, MA). DOC concentrations were determined with a Shimadzu TOC-5000 Analyzer (Shimadzu Corp., Kyoto, Japan). Concentrations of copper and zinc were determined using a Varian 720-ES ICP Optical Emission Spectrometer (Varian Inc., Palo Alto, CA).

3.3 Results and Discussion

3.3.1 Batch P Adsorption Isotherms

The batch P adsorption data was fit to the Langmuir and Freundlich isotherm models and the results are shown in Table 3.2. All three sizes of steel byproducts and the steel slag all fit the Langmuir model well ($R^2 \geq 0.997$), especially compared to the Freundlich model ($0.956 \geq R^2 \geq 0.775$), suggesting that the adsorption of P onto the four materials follows the assumption of monolayer adsorption, where adsorption can only occur at a fixed number of localized sites (Foo and Hameed 2010). Graphically, the Langmuir isotherm is characterized by a plateau or equilibrium saturation where no further adsorption can take place. Figure 3.1 shows the experimental data fitted to the Langmuir model. The predicted P adsorption capacities of the small steel chips, medium steel chips, large steel chips, and steel slag were 4.69, 2.68, 2.13, and 1.48 mg/g, respectively. Between the three sizes of steel byproducts, the adsorption capacities increased with decreasing particle size, likely because of the increase in surface area and

potential adsorption sites at smaller particle sizes. This has been reported in previous research investigating multiple material sizes (Lyngsie et al. 2014; Vohla et al. 2011). Compared to steel slag, medium steel chips exhibited an adsorption capacity 1.8 times greater at a similar size range (2.0-4.8 mm). The adsorption of P onto another similar Fe-based product, iron oxide tailings, was studied by Zeng et al. (2004) in a batch experiment, finding the material to have a P adsorption capacity of 8.21 mg/g. Additionally, Fu et al. (2013) found goethite, a stable Fe oxide, to have a P adsorption capacity of 4.43 mg/g, similar to the results found in this experiment.

3.3.2 Initial Column Experiment

An initial column experiment subjected the four materials to 10.0 mg P/L solution adjusted to pH 7.0 that was pumped upward at a flow rate of 5.89 mL/min (EBCT = 3 min) for 4800 empty bed volumes (10 d). The breakthrough curves of the three sizes of steel byproducts and steel slag are shown Figure 3.2 (a). The steel byproducts all have an immediate breakthrough of P, reaching initial removal rates of 47%, 37%, and 20% for small steel chips, medium steel chips, and large steel chips respectively. All three curves are then characterized by a slow decrease in P removal efficiency over the course of 4800 treated bed volumes. However, none of the three materials reached full exhaustion (C/C_0 = 1.0). It is possible that this is a result of the continuous regeneration of adsorption sites due to continuous oxidation in the column, forming new Fe oxides for P to bind with. In contrast, the adsorption of P onto steel slag demonstrated a traditional S-shaped breakthrough curve and reached complete exhaustion after 1440 empty bed volumes (3 d).

Figure 3.2 (b) shows the cumulative P retained curves of the three sizes of steel byproducts and the steel slag. A positive slope on the cumulative P retained curve indicates that P is adsorbed by the media with a steeper slope indicating higher removal. Once the curve becomes horizontal, the material has become exhausted and no more P removal is taking place. Because only the steel slag reached exhaustion, it is the only curve that is not still increasing after 4800 empty bed volumes. However, because the P removal efficiencies of the steel byproducts are decreasing based on the breakthrough curves, the slopes of the cumulative P retained curves are decreasing as well. After 4800 empty bed volumes, the small steel chips, medium steel chips, large steel chips, and steel slag reached P adsorption capacities of 10.4, 8.43, 9.94, and 1.50 mg/g. Because the steel byproducts did not reach exhaustion during the experiment, the P adsorption capacities calculated are a slight underestimation of the true capacities. Contradictory to the batch study, large steel chips exhibited a higher P adsorption capacity than medium steel chips even while removing less P as shown in the breakthrough curve. Due to the size of large steel chips, the mass needed to pack the column to 10 cm was much less than that of medium steel chips, resulting in a considerably smaller packing density (0.64 g/cm^3). Therefore, the P adsorption capacity on a per mass basis was higher.

Multiple authors have noted a significant difference in the predicted P adsorption capacities between batch and column studies due to the very different conditions of the two techniques (Drizo et al. 2002; Huang et al. 2009; Penn and McGrath 2011). Column adsorption is a dynamic process that continually supplies the materials with fresh reactants. The column P adsorption capacities of the three sizes of steel byproducts in this study were 2.2-4.7 times larger than the batch P adsorption capacities. For steel slag, the

batch and column P adsorption capacities were similar, possibly due to the short EBCT in the column preventing additional P removal via Ca-P precipitation which may have been prevalent with longer reaction times (Penn and McGrath 2011). One of the main P removal mechanism of Fe-based materials (i.e. steel byproducts) is ligand exchange, where the process is much faster compared to precipitation (Allred and Racharaks 2014; Loganathan et al. 2014). Additionally, the formation of new iron-oxides in the column may have led to increased P adsorption capacities.

Steel slag is a material that has been extensively researched by many (Agyei et al. 2002; Drizo et al. 2002; Oguz 2004; Xue et al. 2009) and used for full-scale P removal systems (Penn et al. 2016). However, in this study, steel byproducts appear to be just as promising for P removal, while still maintaining a high hydraulic conductivity. During the experiment, the small steel chips formed multiple masses in the column, which may have limited the hydraulic conductivity and ability for P retention. This raises concern for full-scale treatment, especially during wet and dry cycles. Therefore, medium steel chips were chosen to be studied further based on high P removal efficiencies and optimal size to reduce potential column clogging.

3.3.3 Effect of P Concentration

In order to investigate the effect of initial P concentration of the adsorption of P on medium steel chips, breakthrough and cumulative P retained curves were constructed for 1.0, 10.0, and 50.0 mg P/L solutions adjusted to pH 7.0 pumped upwards at a flow rate of 5.89 mL/min (EBCT = 3 min) for 4800 empty bed volumes (10 d) and are shown in Figure 3.3 (a) and Figure 3.3 (b), respectively. Based on Figure 3.3 (a), it is evident that increasing initial P concentration resulted in faster exhaustion of the material. The

medium steel chips have immediate breakthroughs at all three P concentrations, initially removing 65%, 37%, and 14% for initial P concentrations of 1.0, 10.0, and 50.0 mg/L, respectively. At the low concentration tested (1.0 mg P/L), the medium steel chips exhibited high removal even after 4800 empty bed volumes, removing 40% of the influent P. Because agricultural subsurface drainage is typically lower than 1.0 mg P/L (Algoazany et al. 2007; Fausey et al. 1995; Gentry et al. 2007), the results suggest that greater removal efficiencies could be expected in field conditions. At 50.0 mg P/L, however, the medium steel chips were exhausted after 2880 empty bed volumes (6 d). The calculated P adsorption capacities from the cumulative P retained curves were 2.18, 8.34, and 5.84 mg/g for 1.0, 10.0, and 50.0 mg P/L, respectively. It has been reported that elevating initial P concentrations leads to greater P adsorption capacities (Nguyen et al. 2015; Nur et al. 2014; Sun et al. 2014). However, the tendency for the medium steel chips to continue removing ample amounts of P over 4800 empty bed volumes at 10.0 mg P/L without becoming exhausted led to a higher P adsorption capacity.

3.3.4 Effect of EBCT

The effect of EBCTs of 1 min, 3 min, and 10 min (17.7, 5.89, and 1.77 mL/min) on the adsorption of P onto medium steel chips using a 10.0 mg P/L solution adjusted to pH 7.0 is shown as breakthrough and cumulative P retained curves in Figure 3.4 (a) and Figure 3.4 (b), respectively. Because the experiment length was based on 4800 empty bed volumes, the duration of testing was 3.33 d, 10 d, and 33.3 d. It is clear from the breakthrough curves that shorter EBCTs resulted in lower initial P removal and faster exhaustion times. After initial breakthrough, P removal rates of 20%, 37%, and 42% for EBCTs of 1 min, 3 min, and 10 min were determined. Interestingly, an EBCT of 10 min

resulted in a relatively flat breakthrough curve, consistently removing 41-50% of the influent P for the duration of the experiment. This is likely due to the regeneration of adsorption sites via production of Fe-oxides. It is also possible that the longer retention time in the column could promote for the dissolution of Fe-oxides, which release Fe ions that can form Fe-P precipitates (Allred and Racharaks 2014; Penn and McGrath 2011). The P adsorption capacities of the medium steel chips after 4800 empty bed volumes were 3.52, 8.43, and 22.7 mg/g for EBCTs of 1 min, 3 min, and 10 min, respectively. The consistent removal by the medium steel chips with a 10 min EBCT results in a steep cumulative P retained curve, and the true P adsorption capacity may be much higher. The trend of increasing P adsorption capacities with increasing EBCT (decreasing flow rate) was also observed by Sun et al. (2014) while testing Mg_3-Fe layered double hydroxides. It is likely that the increased EBCT provides for a more efficient interaction between the medium steel chips and P.

3.3.5 Effect of pH

The effect of initial pH on the adsorption of P onto medium steel chips using a 10.0 mg P/L solution pumped upwards at a flow rate of 5.89 mL/min (3 min EBCT) is shown as breakthrough and cumulative P retained curves in Figure 3.5 (a) and Figure 3.5 (b), respectively. Depending on soil type, pH values in agricultural subsurface drainage can be slightly acidic or basic (Fausey et al. 1995; Rozemeijer et al. 2010). To simulate this range, a pH values of 5.0, 7.0, and 9.0 were selected for testing. Initial breakthroughs for the medium steel chips resulted in removal rates of 45%, 37%, and 27% for pH values of 5.0, 7.0, and 9.0, respectively. Although, none of the three columns reached exhaustion, it is clear from both the breakthrough and cumulative P retained curves that

lower pH values led to higher P removal. The P adsorption capacities increased by 56% from pH 9.0 to pH 5.0. In another column study, Nguyen et al. (2015) reported an 34% increase in P adsorption capacity onto zirconium loaded okara. Multiple researches have studied pH impact on P adsorption by Fe-based materials in batch studies and found a similar trend (Fu et al. 2013; Geelhoed et al. 1997; Zeng et al. 2004). The lower P adsorption is likely due to the fact that at higher pH values, the medium steel chips carry more of a negative charge, resulting in an increased repulsion between the medium steel chips and negative phosphate ions. Another explanation may be an increase in adsorption of OH^- ions onto the medium steel chips at high pH values, reducing the amount of potential adsorption sites for P.

3.3.6 Effect of DOC

The installation of woodchip denitrification bioreactors has become an emerging best management practice for nitrate removal from agricultural subsurface drainage (Christianson et al. 2012; Schipper et al. 2010). However, woodchip bioreactors can leach DOC into effluent waters (Healy et al. 2012). In the instance of simultaneous treatment of nitrate and phosphate using woodchip denitrification bioreactors and medium steel chips, the impact of DOC on P adsorption was investigated using a 10.0 mg P/L solution adjusted to pH 7.0 pumped upwards at 5.89 mL/min (3 min EBCT) with coexisting woodchip leached and humic acid derived DOC concentrations of 0, 5.0, and 25.0 mg DOC/L. The breakthrough and cumulative P retained curves of the adsorption of P onto medium steel chips with varying humic acid derived DOC concentrations is shown in Figure 3.6 (a) and Figure 3.6 (b), respectively. The effect of varying woodchip leached DOC is shown in Figure 3.6 (c) and Figure 3.6 (d). The addition of 5.0 and 25.0 mg/L

humic acid derived DOC and woodchip leached DOC had similar adverse effects on the P removal performance by medium steel chips. A coexisting concentration of 25.0 mg/L woodchip leached DOC resulted in the exhaustion of medium steel chips after 4320 empty bed volumes (9 d). Phosphorus adsorption capacities were reduced by 12% and 33% in the presence of 5.0 mg/L and 25.0 mg/L humic acid derived DOC, respectively. Similarly, the presence of 5.0 mg/L and 25.0 mg/L woodchip leached DOC resulted in an 8% and 38% reduction in P adsorption capacity, respectively. Because the reduction of P removal is larger at higher DOC concentrations, it is likely that competitive adsorption between P and DOC onto the medium steel chips is occurring. In a batch study by Weng et al. (2012), the authors reported a reduction in P adsorption onto Fe-oxides of 50% between DOC concentrations of 0.5 to 50.0 mg/L, noting that phosphate ions and DOC are strong competitors for adsorption.

3.3.7 Desorption Potential

In order to investigate the potential of P leaching and P recovery, a 0.01 M KCl solution and three strengths of NaOH solution (0.05 M, 0.10 M, 0.20 M) were passed through columns of exhausted medium steel chips. To determine the potential of P leaching, the 0.01 KCl solution was used to simulate the typical ionic strength of agricultural subsurface drainage. Alternatively, the three NaOH solutions were found to be effective desorption solutions to strip the P off of the medium steel chips. Figure 3.7 shows the percent desorbed from the columns over 120 empty bed volumes (6 h). The addition of the 0.01 KCl solution resulting in trace desorption from the medium steel chips, with < 1% desorbed. This indicates that the chemical bonds formed between Fe and P are strong, reinforcing ligand exchange as the primary P removal mechanism.

Phosphorus recoveries of 59%, 64%, and 83% were found for 0.05 M, 0.10 M, and 0.20 M NaOH solutions, respectively, with a majority of the desorption occurring within 20 empty bed volumes (1 h). Other researchers have found success in reloading adsorption materials with P after sequential desorption experiments, making it a possibility to reuse the medium steel chips after exhaustion (Nur et al. 2014; Sun et al. 2014).

3.3.8 Mixed Contaminant Removal

The ability for medium steel chips to remove additional contaminants was investigated and the results are shown in Figure 3.8. The solution tested consisted of 1.0 mg PO_4^{3-}-P/L, 10.0 mg NO_3^--N /L, 5.0 mg DOC/L, 0.5 mg Cu/L, and 0.5 mg Zn/L, all of which can be present in agricultural subsurface drainage matrixes (Fausey et al. 1995; Healy et al. 2012; Rozemeijer et al. 2010) . Over the duration of 4800 empty bed volumes (10 d), the medium steel chips removed substantial amounts of P, DOC, Cu, and Zn. All of the four constituents were characterized by a fast breakthrough after which removal rates decreased slowly. For the majority of the test, the medium steel chips removed 34-73%, 27-41%, 19-34%, and 13-19% of P, DOC, Cu, and Zn, respectively. The only constituent not reduced considerably was NO_3^--N, with removal rates of only 1-4%. Sun et al. (2014) also reported minimal removal of NO_3^--N in a column study using Mg_3-Fe layered double hydroxides. Other studies have also had success removing Cu and Zn while using Fe-based adsorbents (Reddy et al. 2014; Wu and Zhou 2009). The results of this experiment suggest that medium steel chips may effectively remove additional contaminants from agricultural subsurface drainage while still removing P effectively.

3.3.9 Field-Scale Treatment Recommendations

Steel byproducts are a promising P removal media for agricultural subsurface drainage treatment. The low-cost material has a high P adsorption capacity, while still maintaining a sufficient hydraulic conductivity. To prevent any clogging issues, it is recommended to settle out or sieve the raw material to remove any fine particles (< 2.0 mm) that may solidify and form masses during wet and dry cycles in the field. Before installation, it is also necessary to wash the steel byproducts, removing any oil present on the material surface that may inhibit adsorption. Additionally, air drying the steel byproducts after washing will promote the formation of Fe-oxides on the material surface, increasing the P removal effectiveness. Further research is needed to develop models that can accurately predict the field performance of the steel byproducts. Also, more insight is recommended to determine the potential for recharging the steel byproducts after exhaustion, and examining the ability to recover adsorbed P for reuse.

3.4 Conclusions

Three sizes of steel byproducts and steel slag were tested for P adsorption in batch and column experiments under various conditions to determine their potential for agricultural subsurface drainage treatment. For the batch study, small steel chips, medium steel chips, large steel chips, and steel slag all fit the Langmuir isotherm model well ($R^2 \geq$ 0.997) and had maximum P adsorption capacities of 4.69, 2.68, 2.13, 1.48 mg/g, respectively. In an initial column test, small steel chips, medium steel chips, large steel chips, and steel slag reached P adsorption capacities of 10.4, 8.43, 9.94, and 1.50 mg/g, respectively, indicating higher cumulative P removal in a column setting. Medium steel

chips were chosen for further column testing. An increase in influent P concentration led to faster exhaustion of adsorption sites, while medium steel chips removed lower initial P concentrations more efficiently. Longer EBCTs resulted in higher removal efficiencies and increased cumulative P retained. Increasing initial pH from 5.0 to 9.0 resulted in 56% less cumulative P adsorption onto medium steel chips. The presence of DOC inhibited P adsorption by up to 38%, likely because of competitive adsorption. P recoveries of 59%, 64%, and 83% were measured using 0.05 M, 0.10 M, and 0.20 M NaOH solutions, respectively, with a majority of the desorption occurring within 1 h. Medium steel chips removed considerable amounts of P, DOC, Cu, and Zn in a mixed contaminants matrix. Based on high P adsorption capacities and high hydraulic conductivity, steel byproducts are a promising low-cost adsorbent to be used for treating agricultural subsurface drainage.

Table 3.1: Characteristics of steel byproducts and steel slag.

Material	Size[a] (mm)	Particle Density (g/cm^3)	pH[b]	Packing Density (g/cm^3)	Hydraulic Conductivity (cm/s)
Small Steel Chips	0.1-2.0	5.20	6.3	1.40	0.31
Medium Steel Chips	2.0-4.8	5.50	6.3	1.13	2.44
Large Steel Chips	10-20	5.54	6.3	0.64	3.24
Steel Slag	2.0-4.8	3.57	10.9	1.80	1.01

[a] Size ranges determined from known sieve sizes except for large steel chips, which were measured manually.

[b] Values of pH were obtained from a 1:1 by weight slurry mixture of material and distilled water.

Table 3.2: Langmuir and Freundlich isotherm constants for the adsorption of P onto steel byproducts and steel slag.

Material	Langmuir Isotherm			Freundlich Isotherm		
	q_{max} (mg/g)	K_L (L/mg)	R^2	K_F	n	R^2
Small Steel Chips	4.69	10.6	0.999	9.52	21.5	0.910
Medium Steel Chips	2.68	13.1	0.997	6.34	10.9	0.775
Large Steel Chips	2.13	11.5	0.999	3.61	10.4	0.956
Steel Slag	1.48	2.92	0.998	1.27	9.46	0.899

*****Experimental conditions: initial PO_4^{3-}-P=10.0-40.0 mg/L; pH=7.0; temperature=20 °C; adsorption time=24 h.

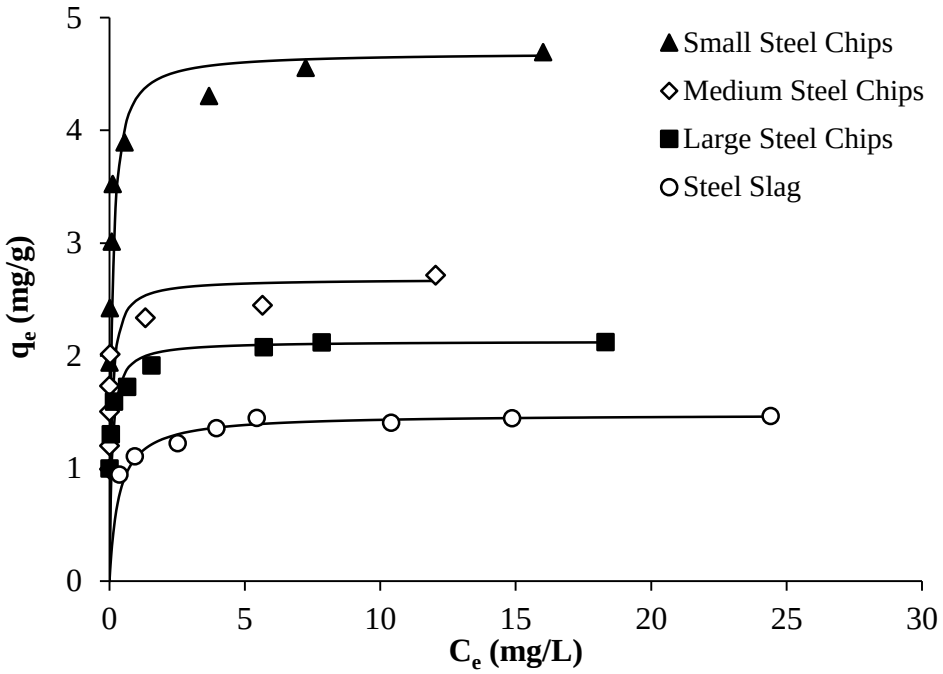

Figure 3.1: Batch Langmuir adsorption isotherms for steel byproducts and steel slag. (Experimental conditions: initial PO_4^{3-}-P=10.0-40.0 mg/L; pH=7.0; temperature=20 °C; adsorption time=24 h.)

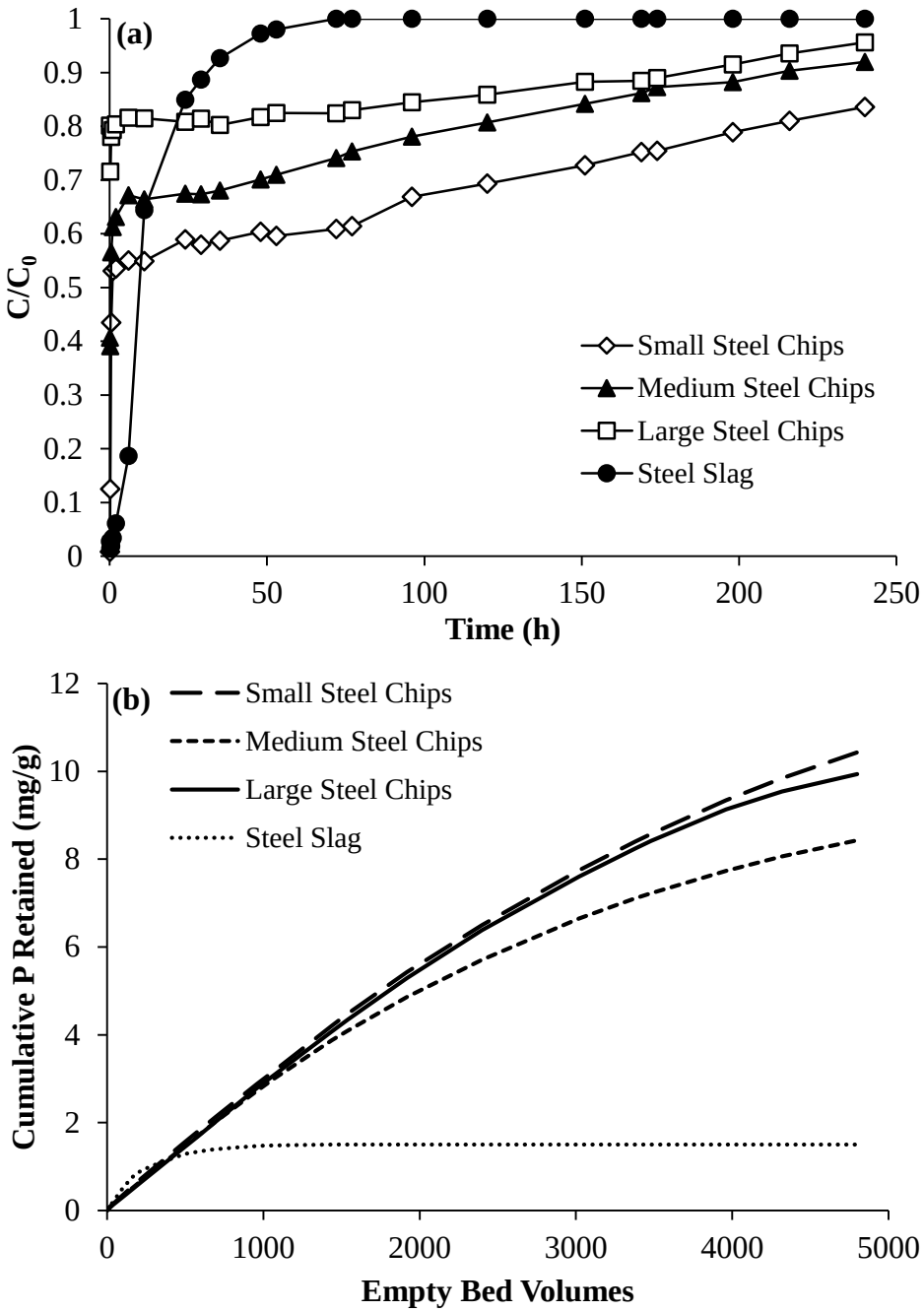

Figure 3.2: Flow-through P adsorption onto steel byproducts and steel slag. (Experimental conditions: influent PO_4^{3-}-P=10.0 mg/L; bed height=10 cm; EBCT=3 min; pH=7.0; duration=10 d). (a) Breakthrough curves of adsorbents. (b) Cumulative P retained by adsorbents.)

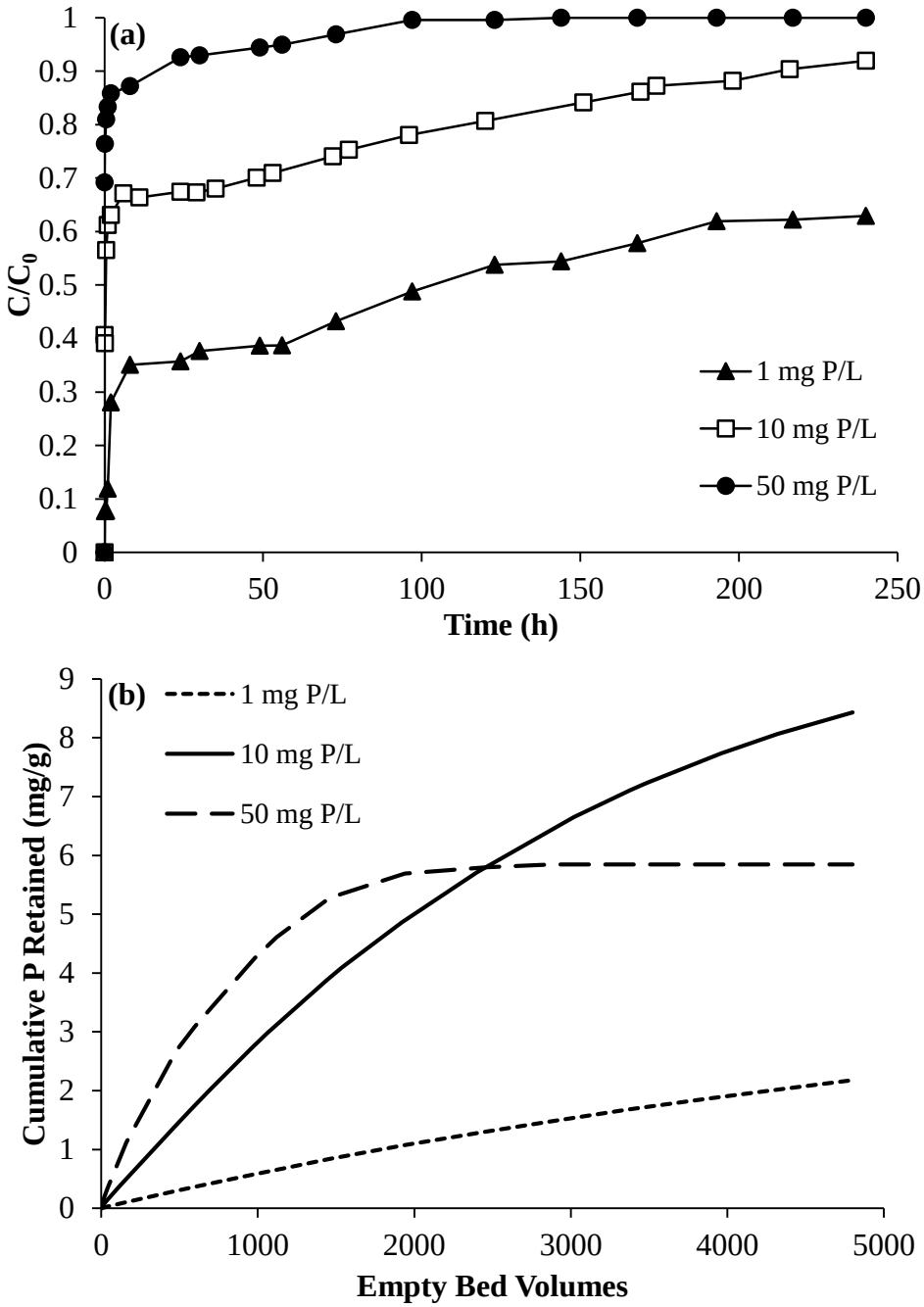

Figure 3.3: Effect of P concentration on adsorption onto medium steel chips. (Experimental conditions: bed height=10 cm; EBCT=3 min; pH=7.0; duration=10 d). (a) Breakthrough curves of medium steel chips. (b) Cumulative P retained by medium steel chips.)

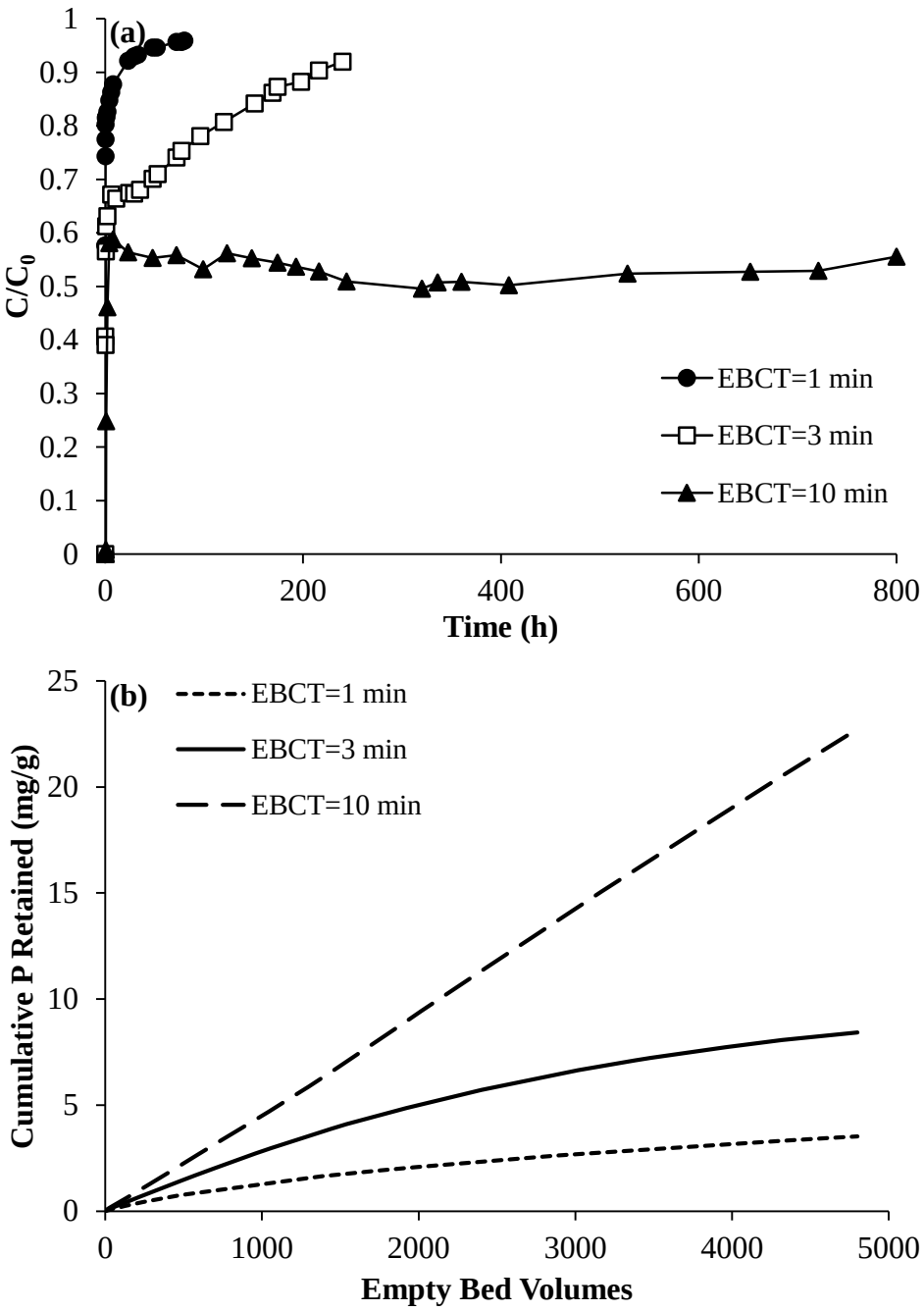

Figure 3.4: Effect of EBCT on P adsorption onto medium steel chips. (Experimental conditions: influent PO_4^{3-}-P=10.0 mg/L; bed height=10 cm; pH=7.0). (a) Breakthrough curves of medium steel chips. (b) Cumulative P retained by medium steel chips.)

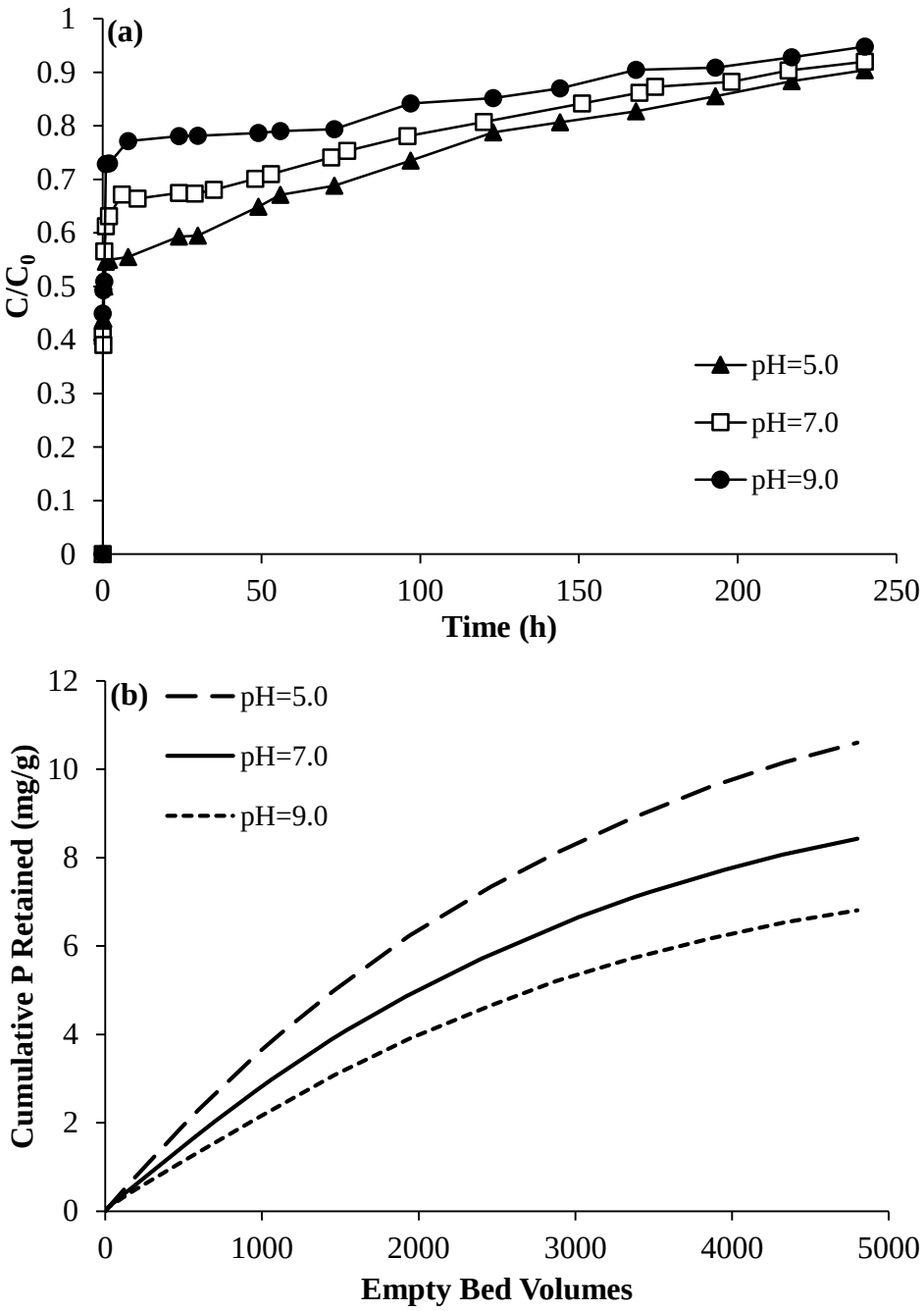

Figure 3.5: Effect of influent pH on P adsorption onto medium steel chips.
(Experimental conditions: influent PO_4^{3-}-P=10.0 mg/L; bed height=10 cm; EBCT=3 min; duration=10 d). (a) Breakthrough curves of medium steel chips. (b) Cumulative P retained by medium steel chips.)

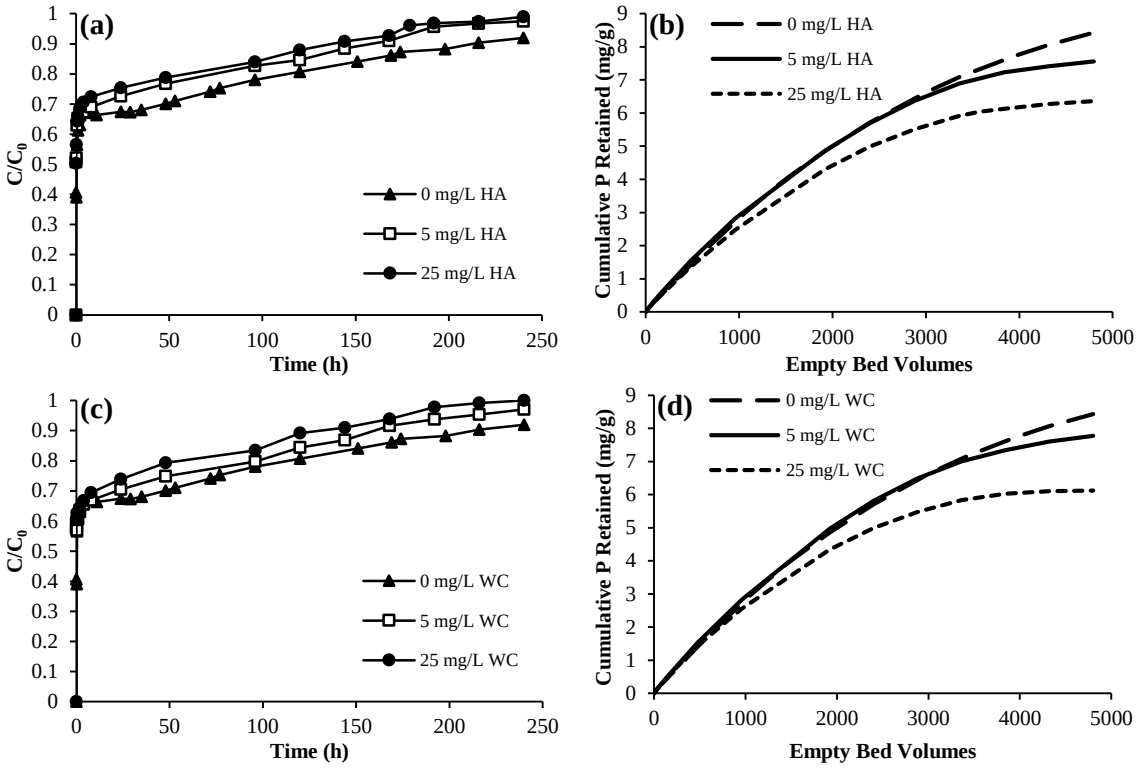

Figure 3.6: Effect of DOC on P adsorption onto medium steel chips. (Experimental conditions: influent PO_4^{3-}-P=10.0 mg/L; bed height=10 cm; EBCT=3 min; pH=7.0; duration=10 d). (a) Humic acid DOC breakthrough curves. (b) Humic acid DOC cumulative P retained. (c) Woodchip leached DOC breakthrough curves. (d) Woodchip leached DOC cumulative P retained.)

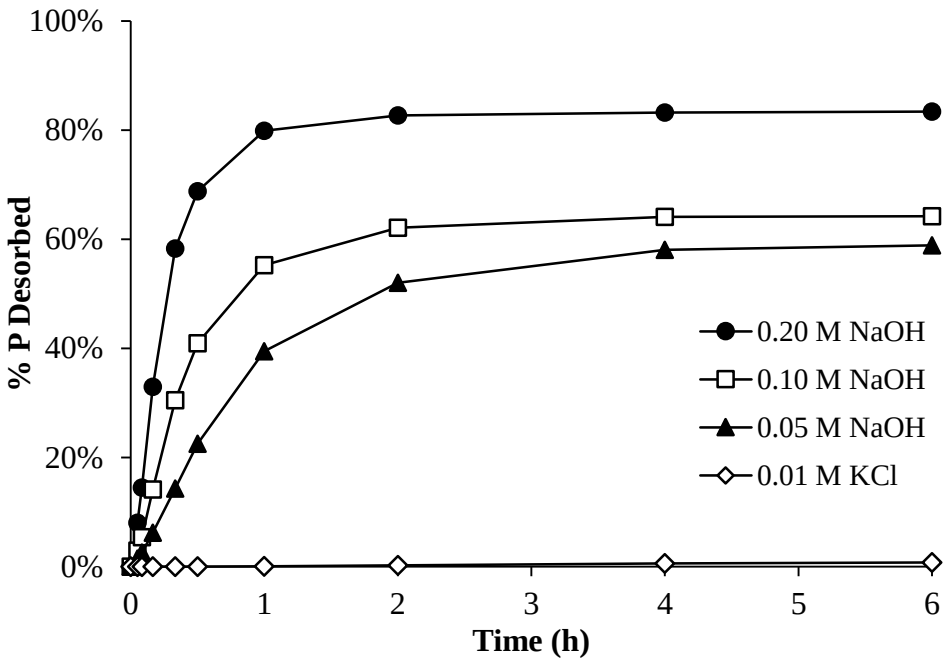

Figure 3.7: Desorption of P from medium steel chips. (Experimental conditions: bed height=10 cm; EBCT=3 min.)

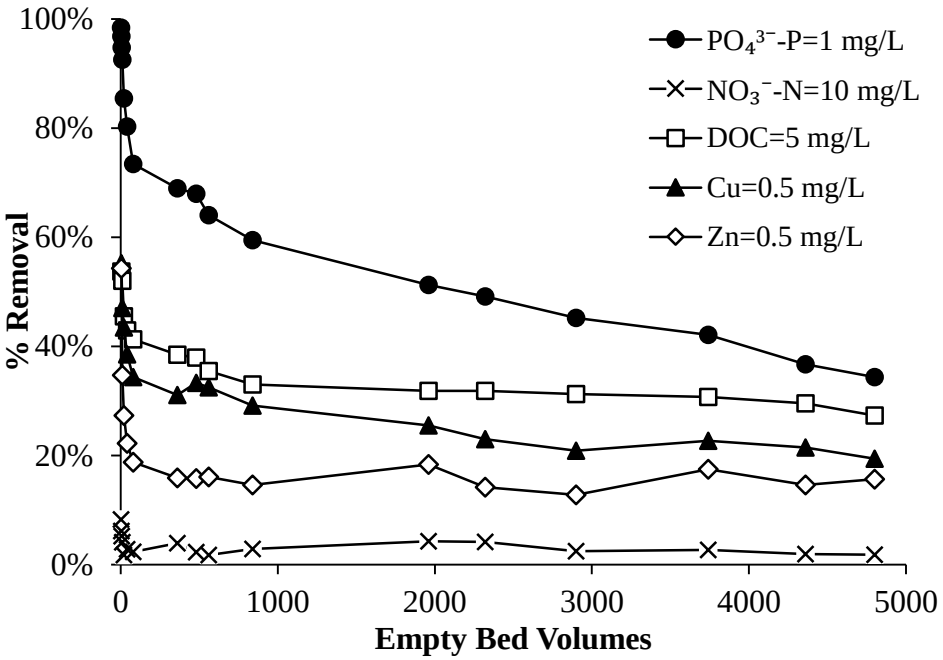

Figure 3.8: Removal of mixed contaminants by medium steel chips. (Experimental conditions: bed height=10 cm; EBCT=3 min; pH=7.0; duration=10 d).

CHAPTER 4

SUMMARY AND RECOMMENDATIONS

Phosphorus (P) adsorption batch tests were performed using three natural minerals (limestone, zeolite, and calcite) and five industrial byproducts (steel slag, iron filings, and three sizes of steel byproducts). The industrial byproducts exhibited substantially higher adsorption capacities than the natural minerals, ranging from 1.68 to 4.95 mg/g compared to 0.10 to 0.13 mg/g at 20 °C. The three sizes of steel byproducts exhibited P adsorption capacities of 2.54 to 4.47 mg/g, which were comparable to steel slag and the iron filings. Increasing temperature resulted in 1.2 to 2.8 times larger P adsorption capacities between 30 °C and 5 °C. Decreasing pH resulted in an increase in adsorption among the steel byproducts. The presence of varying concentrations of coexisting anions nitrate and sulfate had little impact on P removal. However, increasing concentrations of DOC inhibited P adsorption by up to 24% for steel byproducts.

A fixed-bed column experiment and initial batch test were performed using steel slag and three sizes of steel byproducts. For the batch study, small steel chips, medium steel chips, large steel chips, and steel slag had maximum P adsorption capacities of 4.69, 2.68, 2.13, 1.48 mg/g, respectively. For the column test, small steel chips, medium steel chips, large steel chips, and steel slag reached P adsorption capacities of 10.4, 8.43, 9.94, and 1.50 mg/g, respectively, indicating higher cumulative P removal in a column setting. Medium steel chips were chosen for additional column testing. An increase in influent P concentration led to faster exhaustion of adsorption sites, while medium steel chips removed lower initial P concentrations more efficiently. Longer EBCTs resulted in higher removal efficiencies and increased cumulative P retained. An increase in initial pH from

5.0 to 9.0 resulted in 56% less cumulative P adsorption onto medium steel chips. The presence of DOC inhibited P adsorption by up to 38%. P recoveries of 59%, 64%, and 83% were measured using 0.05 M, 0.10 M, and 0.20 M NaOH solutions, respectively, with a majority of the desorption occurring within 1 h. Medium steel chips removed considerable amounts of P, DOC, Cu, and Zn in a mixed contaminants matrix.

Overall, based on high P adsorption capacities under various conditions in batch and column studies, steel byproducts are a promising low-cost adsorbent that is recommended for agricultural subsurface drainage treatment. To further understand and predict field-scale P removal performance using steel byproducts, the development of an empirical model is recommended. Additional research to determine the potential of P recovery from steel byproducts in order to recharge the material may help extend the longevity of a potential P removal structure.

LIST OF REFERENCES

Adam, K., Krogstad, T., Vråle, L., Søvik, A. K., and Jenssen, P. D. (2007). "Phosphorus retention in the filter materials shellsand and Filtralite P®—Batch and column experiment with synthetic P solution and secondary wastewater." *Ecological Engineering*, 29(2), 200-208.

Agyei, N. M., Strydom, C., and Potgieter, J. (2002). "The removal of phosphate ions from aqueous solution by fly ash, slag, ordinary Portland cement and related blends." *Cement and concrete research*, 32(12), 1889-1897.

Algoazany, A. S., Kalita, P. K., Czapar, G. F., and Mitchell, J. K. (2007). "Phosphorus transport through subsurface drainage and surface runoff from a flat watershed in east central Illinois, USA." *Journal of Environmental Quality*, 36(3), 681-693.

Allred, B. J., and Racharaks, R. (2014). "Laboratory comparison of four iron-based filter materials for drainage water phosphate treatment." *Water Environment Research*, 86(9), 852-862.

Baker, J., Campbell, K., Johnson, H., and Hanway, J. (1975). "Nitrate, phosphorus, and sulfate in subsurface drainage water." *Journal of Environmental Quality*, 4(3), 406-412.

Buda, A. R., Koopmans, G. F., Bryant, R. B., and Chardon, W. J. (2012). "Emerging technologies for removing nonpoint phosphorus from surface water and groundwater: Introduction." *Journal of Environmental Quality*, 41(3), 621-627.

Cameron, S. G., and Schipper, L. A. (2010). "Nitrate removal and hydraulic performance of organic carbon for use in denitrification beds." *Ecological Engineering*, 36(11), 1588-1595.

Chardon, W. J., Groenenberg, J. E., Temminghoff, E. J., and Koopmans, G. F. (2012). "Use of reactive materials to bind phosphorus." *Journal of environmental quality*, 41(3), 636-646.

Christianson, L. E., Bhandari, A., and Helmers, M. J. (2012). "A practice-oriented review of woodchip bioreactors for subsurface agricultural drainage." *Applied engineering in agriculture*, 28(6), 861.

Claytor, R. A., and Schueler, T. R. (1996). *Design of stormwater filtering systems*, Chesapeake Research Consortium.

Correll, D. L. (1998). "The role of phosphorus in the eutrophication of receiving waters: A review." *Journal of Environmental Quality*, 27(2), 261-266.

Cucarella, V., and Renman, G. (2009). "Phosphorus sorption capacity of filter materials used for on-site wastewater treatment determined in batch experiments–a comparative study." *Journal of environmental quality*, 38(2), 381-392.

Drizo, A., Comeau, Y., Forget, C., and Chapuis, R. P. (2002). "Phosphorus saturation potential: A parameter for estimating the longevity of constructed wetland systems." *Environmental science & technology*, 36(21), 4642-4648.

Eidman, V. R. (1997). "Minnesota farmland drainage: Profitability and concerns."

Erickson, A. J., Gulliver, J. S., and Weiss, P. T. (2007). "Enhanced sand filtration for storm water phosphorus removal." *Journal of Environmental Engineering*, 133(5), 485-497.

Erickson, A. J., Gulliver, J. S., and Weiss, P. T. (2012). "Capturing phosphates with iron enhanced sand filtration." *Water research*, 46(9), 3032-3042.

Fausey, N. R., Brown, L. C., Belcher, H. W., and Kanwar, R. S. (1995). "Drainage and water quality in Great Lakes and cornbelt states." *Journal of Irrigation and Drainage Engineering*, 121(4), 283-288.

Foo, K. Y., and Hameed, B. H. (2010). "Insights into the modeling of adsorption isotherm systems." *Chemical Engineering Journal*, 156(1), 2-10.

Fu, Z., Wu, F., Song, K., Lin, Y., Bai, Y., Zhu, Y., and Giesy, J. P. (2013). "Competitive interaction between soil-derived humic acid and phosphate on goethite." *Applied Geochemistry*, 36, 125-131.

Geelhoed, J. S., Hiemstra, T., and Van Riemsdijk, W. H. (1997). "Phosphate and sulfate adsorption on goethite: single anion and competitive adsorption." *Geochimica et Cosmochimica Acta*, 61(12), 2389-2396.

Gentry, L., David, M., Royer, T., Mitchell, C., and Starks, K. (2007). "Phosphorus transport pathways to streams in tile-drained agricultural watersheds." *Journal of Environmental Quality*, 36(2), 408-415.

Genz, A., Kornmüller, A., and Jekel, M. (2004). "Advanced phosphorus removal from membrane filtrates by adsorption on activated aluminium oxide and granulated ferric hydroxide." *Water research*, 38(16), 3523-3530.

Grace, M. A., Healy, M. G., and Clifford, E. (2015). "Use of industrial by-products and natural media to adsorb nutrients, metals and organic carbon from drinking water." *Science of The Total Environment*, 518, 491-497.

Griffin, R., and Jurinak, J. (1973). "The interaction of phosphate with calcite." *Soil Science Society of America Journal*, 37(6), 847-850.

Hansen, N. C., Daniel, T., Sharpley, A., and Lemunyon, J. (2002). "The fate and transport of phosphorus in agricultural systems." *Journal of Soil and Water Conservation*, 57(6), 408-417.

Healy, M. G., Ibrahim, T. G., Lanigan, G. J., Serrenho, A. J., and Fenton, O. (2012). "Nitrate removal rate, efficiency and pollution swapping potential of different organic carbon media in laboratory denitrification bioreactors." *Ecological Engineering*, 40, 198-209.

Heathwaite, A., and Dils, R. (2000). "Characterising phosphorus loss in surface and subsurface hydrological pathways." *Science of the Total Environment*, 251, 523-538.

Huang, X., Liao, X., and Shi, B. (2009). "Adsorption removal of phosphate in industrial wastewater by using metal-loaded skin split waste." *Journal of hazardous materials*, 166(2), 1261-1265.

Hussain, S., Aziz, H. A., Isa, M. H., Ahmad, A., Van Leeuwen, J., Zou, L., Beecham, S., and Umar, M. (2011). "Orthophosphate removal from domestic wastewater using limestone and granular activated carbon." *Desalination*, 271(1), 265-272.

Karageorgiou, K., Paschalis, M., and Anastassakis, G. N. (2007). "Removal of phosphate species from solution by adsorption onto calcite used as natural adsorbent." *Journal of Hazardous Materials*, 139(3), 447-452.

King, K. W., Williams, M. R., and Fausey, N. R. (2015). "Contributions of systematic tile drainage to watershed-scale phosphorus transport." *Journal of environmental quality*, 44(2), 486-494.

King, K. W., Williams, M. R., Macrae, M. L., Fausey, N. R., Frankenberger, J., Smith, D. R., Kleinman, P. J., and Brown, L. C. (2015). "Phosphorus transport in agricultural subsurface drainage: A review." *Journal of environmental quality*, 44(2), 467-485.

Lalley, J., Han, C., Li, X., Dionysiou, D. D., and Nadagouda, M. N. (2016). "Phosphate adsorption using modified iron oxide-based sorbents in lake water: kinetics, equilibrium, and column tests." *Chemical Engineering Journal*, 284, 1386-1396.

Lawlor, P. A., Helmers, M. J., Baker, J. L., Melvin, S. W., and Lemke, D. W. (2008). "Nitrogen application rate effect on nitrate-nitrogen concentration and loss in subsurface drainage for a corn-soybean rotation." *Transactions of the ASABE*, 51(1), 83-94.

Loganathan, P., Vigneswaran, S., Kandasamy, J., and Bolan, N. S. (2014). "Removal and recovery of phosphate from water using sorption." *Critical Reviews in Environmental Science and Technology*, 44(8), 847-907.

Lyngsie, G., Borggaard, O. K., and Hansen, H. C. B. (2014). "A three-step test of phosphate sorption efficiency of potential agricultural drainage filter materials." *Water research*, 51, 256-265.

McDowell, R., Sharpley, A., and Bourke, W. (2008). "Treatment of drainage water with industrial by-products to prevent phosphorus loss from tile-drained land." *Journal of environmental quality*, 37(4), 1575-1582.

Mezenner, N. Y., and Bensmaili, A. (2009). "Kinetics and thermodynamic study of phosphate adsorption on iron hydroxide-eggshell waste." *Chemical Engineering Journal*, 147(2-3), 87-96.

Nguyen, T., Ngo, H., Guo, W., Pham, T., Li, F., Nguyen, T., and Bui, X. (2015). "Adsorption of phosphate from aqueous solutions and sewage using zirconium loaded okara (ZLO): fixed-bed column study." *Science of the Total Environment*, 523, 40-49.

Nur, T., Johir, M., Loganathan, P., Nguyen, T., Vigneswaran, S., and Kandasamy, J. (2014). "Phosphate removal from water using an iron oxide impregnated strong base anion exchange resin." *Journal of Industrial and Engineering Chemistry*, 20(4), 1301-1307.

Oguz, E. (2004). "Removal of phosphate from aqueous solution with blast furnace slag." *Journal of Hazardous Materials*, 114(1), 131-137.

Onyango, M. S., Kuchar, D., Kubota, M., and Matsuda, H. (2007). "Adsorptive removal of phosphate ions from aqueous solution using synthetic zeolite." *Industrial & Engineering Chemistry Research*, 46(3), 894-900.

Penn, C., Bowen, J., McGrath, J., Nairn, R., Fox, G., Brown, G., Wilson, S., and Gill, C. (2016). "Evaluation of a universal flow-through model for predicting and designing phosphorus removal structures." *Chemosphere*, 151, 345-355.

Penn, C., Bryant, R., Callahan, M., and McGrath, J. (2011). "Use of industrial by-products to sorb and retain phosphorus." *Communications in Soil Science and Plant Analysis*, 42(6), 633-644.

Penn, C., McGrath, J., Bowen, J., and Wilson, S. (2014). "Phosphorus removal structures: A management option for legacy phosphorus." *Journal of Soil and Water Conservation*, 69(2), 51A-56A.

Penn, C. J., and McGrath, J. M. (2011). "Predicting phosphorus sorption onto steel slag using a flow-through approach with application to a pilot scale system." *Journal of Water Resource and Protection*, 3(4), 235.

Perassi, I., and Borgnino, L. (2014). "Adsorption and surface precipitation of phosphate onto CaCO 3–montmorillonite: effect of pH, ionic strength and competition with humic acid." *Geoderma*, 232, 600-608.

Reddy, K. R., Xie, T., and Dastgheibi, S. (2014). "Nutrients removal from urban stormwater by different filter materials." *Water, Air, & Soil Pollution*, 225(1), 1-14.

Rozemeijer, J., Van der Velde, Y., Van Geer, F., Bierkens, M., and Broers, H. (2010). "Direct measurements of the tile drain and groundwater flow route contributions to surface water contamination: From field-scale concentration patterns in groundwater to catchment-scale surface water quality." *Environmental Pollution*, 158(12), 3571-3579.

Saha, P., and Chowdhury, S. (2011). *Insight into adsorption thermodynamics*, INTECH Open Access Publisher.

Schindler, D. W., Hecky, R. E., Findlay, D. L., Stainton, M. P., Parker, B. R., Paterson, M. J., Beaty, K. G., Lyng, M., and Kasian, S. E. M. (2008). "Eutrophication of lakes cannot be controlled by reducing nitrogen input: Results of a 37-year whole-ecosystem experiment." *Proceedings of the National Academy of Sciences of the United States of America*, 105(32), 11254-11258.

Schipper, L. A., Robertson, W. D., Gold, A. J., Jaynes, D. B., and Cameron, S. C. (2010). "Denitrifying bioreactors—an approach for reducing nitrate loads to receiving waters." *Ecological engineering*, 36(11), 1532-1543.

Sharpley, A., and Tunney, H. (2000). "Phosphorus research strategies to meet agricultural and environmental challenges of the 21st century." *Journal of Environmental Quality*, 29(1), 176-181.

Sharpley, A. N., Chapra, S., Wedepohl, R., Sims, J., Daniel, T. C., and Reddy, K. (1994). "Managing agricultural phosphorus for protection of surface waters: Issues and options." *Journal of environmental quality*, 23(3), 437-451.

Sims, J., Simard, R., and Joern, B. (1998). "Phosphorus loss in agricultural drainage: Historical perspective and current research." *Journal of Environmental Quality*, 27(2), 277-293.

Skaggs, R. W., Breve, M. A., and Gilliam, J. W. (1994). "HYDROLOGIC AND WATER-QUALITY IMPACTS OF AGRICULTURAL DRAINAGE." *Critical Reviews in Environmental Science and Technology*, 24(1), 1-32.

Smith, D. R., King, K. W., Johnson, L., Francesconi, W., Richards, P., Baker, D., and Sharpley, A. N. (2015). "Surface Runoff and Tile Drainage Transport of Phosphorus in the Midwestern United States." *Journal of Environmental Quality*, 44(2), 495-502.

Sonzogni, W., Chapra, S., Armstrong, D., and Logan, T. (1982). "Bioavailability of phosphorus inputs to lakes." *Journal of Environmental Quality*, 11(4), 555-563.

Stoner, D., Penn, C., McGrath, J., and Warren, J. (2012). "Phosphorus removal with by-products in a flow-through setting." *Journal of environmental quality*, 41(3), 654-663.

Sun, X., Imai, T., Sekine, M., Higuchi, T., Yamamoto, K., Kanno, A., and Nakazono, S. (2014). "Adsorption of phosphate using calcined Mg 3–Fe layered double hydroxides in a fixed-bed column study." *Journal of Industrial and Engineering Chemistry*, 20(5), 3623-3630.

Vohla, C., Kõiv, M., Bavor, H. J., Chazarenc, F., and Mander, Ü. (2011). "Filter materials for phosphorus removal from wastewater in treatment wetlands—A review." *Ecological Engineering*, 37(1), 70-89.

Warneke, S., Schipper, L. A., Bruesewitz, D. A., McDonald, I., and Cameron, S. (2011). "Rates, controls and potential adverse effects of nitrate removal in a denitrification bed." *Ecological engineering*, 37(3), 511-522.

Weng, L., Van Riemsdijk, W. H., and Hiemstra, T. (2012). "Factors controlling phosphate interaction with iron oxides." *Journal of environmental quality*, 41(3), 628-635.

Wu, P., and Zhou, Y.-s. (2009). "Simultaneous removal of coexistent heavy metals from simulated urban stormwater using four sorbents: a porous iron sorbent and its mixtures with zeolite and crystal gravel." *Journal of hazardous materials*, 168(2), 674-680.

Xue, Y., Hou, H., and Zhu, S. (2009). "Characteristics and mechanisms of phosphate adsorption onto basic oxygen furnace slag." *Journal of Hazardous Materials*, 162(2), 973-980.

Zeng, L., Li, X., and Liu, J. (2004). "Adsorptive removal of phosphate from aqueous solutions using iron oxide tailings." *Water Research*, 38(5), 1318-1326.

Zhang, T. Q., Tan, C. S., Zheng, Z. M., and Drury, C. F. (2015). "Tile Drainage Phosphorus Loss with Long-Term Consistent Cropping Systems and Fertilization." *Journal of Environmental Quality*, 44(2), 503-511.

Zucker, L. A., and Brown, L. C. (1998). *Agricultural drainage: Water quality impacts and subsurface drainage studies in the Midwest*, Ohio State University Extension.